

DART: Diversify-Aggregate-Repeat Training Improves Generalization of Neural Networks

Samyak Jain ^{*} ^{◊‡} Sravanti Addepalli ^{*} [†] Pawan Sahu [‡] ^{§‡} Priyam Dey [‡] [†] R.V. Babu [†]
[†] Video Analytics Lab, Indian Institute of Science, Bangalore
[◊] Indian Institute of Technology, Varanasi [§] Indian Institute of Technology, Dhanbad

Abstract

Generalization of Neural Networks is crucial for deploying them safely in the real world. Common training strategies to improve generalization involve the use of data augmentations, ensembling and model averaging. In this work, we first establish a surprisingly simple but strong benchmark for generalization which utilizes diverse augmentations within a training minibatch, and show that this can learn a more balanced distribution of features. Further, we propose Diversify-Aggregate-Repeat Training (DART) strategy that first trains diverse models using different augmentations (or domains) to explore the loss basin, and further Aggregates their weights to combine their expertise and obtain improved generalization. We find that Repeating the step of Aggregation throughout training improves the overall optimization trajectory and also ensures that the individual models have a sufficiently low loss barrier to obtain improved generalization on combining them. We shed light on our approach by casting it in the framework proposed by Shen et al. [61] and theoretically show that it indeed generalizes better. In addition to improvements in In-Domain generalization, we demonstrate SOTA performance on the Domain Generalization benchmarks in the popular DomainBed framework as well. Our method is generic and can easily be integrated with several base training algorithms to achieve performance gains.

1. Introduction

Deep Neural Networks have outperformed classical methods in several fields and applications owing to their remarkable generalization. Classical Machine Learning theory assumes that test data is sampled from the same distribution as train data. This is referred to as the problem of In-Domain (ID) generalization [16, 19, 30, 34, 52], where the goal of the model is to generalize to samples within

^{*}Equal Contribution. [‡] Equal contribution second authors. Correspondence to Samyak Jain <samyakjain.cse18@iitbhu.ac.in>, Sravanti Addepalli <sravantia@iisc.ac.in>. [†] Work done during internship at Video Analytics Lab, Indian Institute of Science, Bangalore.

same domain as the train dataset. This is often considered to be one of the most important requirements and criteria to evaluate models. However, in several cases, the test distribution may be different from the train distribution. For example, surveillance systems are expected to work well at all times of the day, under different lighting conditions and when there are occlusions. However, it may not be possible to train models using data from all these distributions. It is therefore crucial to train models that are robust to distribution shifts, which is popularly referred to as Out-of-Domain (OOD) Generalization [26]. In this work, we consider the problems of In-Domain generalization and Out-of-Domain Generalization of Deep Networks. For the latter case, we consider the popular setting of Domain Generalization [6, 24, 45], where the training data is assumed to be composed of several source domains and the goal is to generalize to an unseen target domain.

The problem of generalization is closely related to the Simplicity Bias of Neural Networks, due to which models have a tendency to rely on simpler features that are often spurious correlations to the labels, when compared to the harder robust features [59]. For example, models tend to rely on weak features such as background, rather than more robust features such as shape, causing a drop in object classification accuracy when background changes [23, 76].

A common strategy to alleviate this is to use data augmentations [10–12, 28, 46, 56, 79, 81] or data from several domains during training [24], which can result in invariance to several spurious correlations, improving the generalization of models. Shen et al. [61] show that data augmentations enable the model to give higher importance to harder-to-learn robust features by delaying the learning of spurious features. We extend their observation by showing that training on a combination of several augmentation strategies (which we refer to as *Mixed* augmentation) can result in the learning of a balanced distribution of diverse features. Using this, we obtain a strong benchmark for ID generalization as shown in Table-1. However, as shown in prior works [1], the impact of augmentations in training is limited by the capacity of the network in being able to

Table 1. **Motivation:** Performance (%) on CIFAR100, ResNet-18 with ERM training for 200 epochs across different train and test augmentations. Mixed-Training (MT) outperforms individual augmentations, while ensembles perform best on average.

Train	Test			
	No Aug.	Cutout	Cutmix	AutoAugment
Pad+Crop+HFlip (PC)	78.51	67.04	56.52	58.33
Cutout (CO)	77.99	74.58	56.12	58.47
Cutmix (CM)	80.54	74.05	77.35	61.23
AutoAugment (AA)	79.18	71.26	60.97	73.91
Mixed-Training (MT)	81.43	77.31	73.20	74.73
Ensemble (CM+CO+AA)	83.61	79.19	73.19	73.90

generalize well to the diverse augmented data distribution. Therefore, increasing the diversity of training data demands the use of larger model capacities to achieve optimal performance. This demand for higher model capacity can be mitigated by training specialists on each kind of augmentation and ensembling their outputs [13, 40, 63, 83], which results in improved performance as shown in Table-1. Another generic strategy that is known to improve generalization is model-weight averaging [33, 74, 75]. This results in a flatter minima, thereby improving the robustness to distribution shifts.

In this work, we aim to combine the benefits of the three strategies discussed above - diversification, specialization and model weight averaging, while also overcoming their individual shortcomings. We propose a **Diversify-Aggregate-Repeat** Training strategy dubbed DART (Fig.1), that first trains k *Diverse* models after a few epochs of common training, and then *Aggregates* their weights to obtain a single generalized solution. The aggregated model is then used to reinitialize the k models which are trained further post aggregation. This process is *Repeated* over training to obtain improved generalization. The *Diversify* step allows models to explore the loss basin and specialize on a fixed set of features. The *Aggregate* (or Model Interpolation) step robustly combines these models, increasing the diversity of represented features while also suppressing spurious correlations. Repeating the *Diversify-Aggregate* steps over training results in a more robust optimization trajectory and also ensures that the k diverse models remain in the same basin thereby permitting a fruitful combination of their weights. We justify our approach theoretically and empirically, and also show that the intermediate model aggregation not only ensures that the models are in the same basin, but also increases the learning time for spurious features, improving generalization. We present our key contributions below.

- We present a strong baseline termed Mixed-Training (MT) that uses a combination of diverse augmentations for different images in a training minibatch.
- We propose a novel algorithm DART, that learns specialized diverse models and aggregates their weights iteratively to improve generalization.

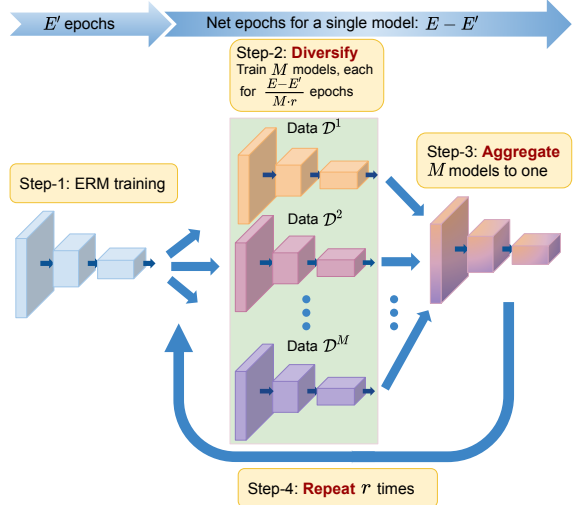


Figure 1. Schematic Diagram of the proposed method DART

- We justify our method theoretically, and empirically on several In-Domain (CIFAR-10, CIFAR-100) and Domain Generalization (OfficeHome, PACS, VLCS, TerraIncognita, DomainNet) datasets.

2. Background: Mode Connectivity of Models

The overparameterization of Deep networks leads to the existence of multiple optimal solutions to any given loss function [35, 49, 80]. Prior works [15, 22, 50] have shown that all such solutions learned by SGD lie on a non-linear manifold, and are connected to each other by a path of low loss. Frankle *et al.* [20] further showed that converged models that share a common initial optimization path are linearly connected with a low loss barrier. This is referred to as the *linear mode connectivity* between the models. Several optimal solutions that are linearly connected to each other are said to belong to a common *basin* which is separated from other regions of the loss landscape with a higher loss barrier. Loss barrier between any two models θ_1 and θ_2 is defined as the maximum loss that can be attained by the models, $\hat{\theta} = \alpha \cdot \theta_1 + (1 - \alpha) \cdot \theta_2 \quad \forall \alpha \in [0, 1]$.

The linear mode connectivity of models facilitates the averaging of weights of different models in a common basin resulting in further gains. In this work, we leverage the linear mode connectivity of diverse models trained from a common initialization to improve generalization.

3. Related Works

3.1. Generalization of Deep Networks

Prior works aim to improve the generalization of Deep Networks by imposing invariances to several factors of variation. This is achieved by using data augmentations during training to improve the In-Domain generalization [10–12, 27, 46, 69, 79, 81], or by training on a combination of multiple domains for Domain Generalization [9, 29, 32, 42, 45].

Contrary to these methods, several works focused on utilizing domain-specific features [5, 14], while others try to disentangle the features into domain-specific and domain-invariant for better generalization [8, 36, 42, 53, 72]. Data augmentation has also been exploited for Domain Generalization [47, 54, 60, 62, 70, 71, 73, 77, 78, 85, 86] in order to increase the diversity of training data and simulate domain shift. Foret *et al.* [19] show that minimizing the maximum loss within an ℓ_2 norm ball of weights can result in a flatter minima thereby improving generalization. Gulrajani *et al.* [24] show that the simple strategy of ERM training on data from several source domains can indeed prove to be a very strong baseline for Domain Generalization. The authors also release DomainBed - which benchmarks several existing methods on some common datasets representing different types of distribution shifts. We empirically show that our method achieves SOTA on the popular Domain Generalization benchmarks and helps in further improving performance and generalization when used in conjunction with several other methods (Table-4) ascribing to its orthogonal nature.

3.2. Averaging model weights across training

Recent works have shown that converging to a flatter minima can lead to improved generalization [16, 19, 30, 34, 52, 64]. Izmailov *et al.* [33] proposed Stochastic Weight Averaging (SWA) to average the model weights from the last few epochs such that the resulting model converges to a flatter minima, thus improving generalization. A variation of SWA, Exponential Moving Average (EMA) of model weights across training iterations is often used to boost model performance at no extra training cost. Cha *et al.* [6] theoretically show that converging to a flatter minima results in a smaller domain generalization gap. The authors propose SWAD that overcomes the limitations of SWA in the Domain Generalization setting and combines several models in the optimal solution basin to obtain a flatter minima with better generalization. We demonstrate that our approach effectively integrates with EMA and SWAD for In-Domain and Domain Generalization settings respectively to obtain further performance gains (Tables-2, 3).

3.3. Averaging weights of fine-tuned models

While earlier works combined models generated from the same optimization trajectory, Tatro *et al.* [66] showed that for any two converged models with different random initializations, one can find a permutation of one of the models so that fine-tuning the interpolation of the second model and the permuted first model leads to improved generalization. On a similar note, Zhao *et al.* [84] proposed to achieve robustness to backdoor attacks by fine-tuning the linear interpolation of pretrained models. More recently, Wortsman *et al.* [75] proposed Model Soups and showed that in a transfer learning setup, fine-tuning and then aver-

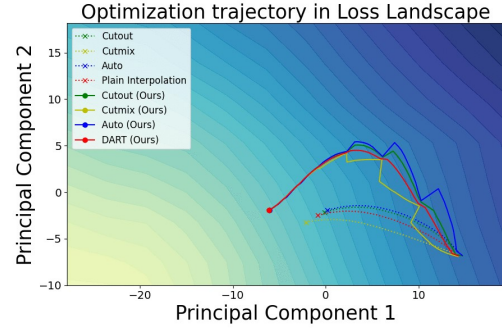


Figure 2. **Optimization trajectory** of the proposed approach DART when compared to independent ERM training on each augmentation. Axes represent the top two PCA directions obtained using the weights of DART training. The initial common point on the right represents the model obtained after 100 epochs of Mixed Training (MT). The trajectory shown is for an additional 100 epochs, with a total training budget of 200 epochs. The optimization trajectory of DART is better aligned with the negative gradient direction when compared to the baseline.

aging different models with same pre-trained initialization but with different hyperparameters such as learning rates, optimizers and augmentations can improve the generalization of the resulting model. The authors further note that this works best when the pre-trained model is trained on a large heterogeneous dataset. While all these approaches work only in a finetuning setting, the proposed method incorporates the interpolation of differently trained models in the regime of *training from scratch*, allowing the learning of models for longer schedules and larger learning rates.

3.4. Averaging weights of differently trained models

Wortsman *et al.* [74] propose to average the weights of multiple models trained with different random initializations simultaneously by considering the loss of a combined model for optimization while performing gradient updates on the individual models. Additionally, they minimize the cosine similarity between model weights to ensure that the models learned are diverse. While this training formulation does learn diverse connected models, it leads to individual models having sub-optimal accuracy (Table-2) since their loss is not optimized directly. DART overcomes such issues since the individual models are trained directly to optimize their respective classification losses. Moreover, the step of intermediate interpolation ensures that the individual models also have better performance when compared to the baseline of standard ERM training on the respective augmentations (Fig.8).

4. Proposed Method: DART

A series of observations from prior works [15, 20, 22, 50] have led to the conjecture that models trained independently with different initializations could be linearly connected

Algorithm 1 Diversify-Aggregate-Repeat Training, DART

```

1: Input:  $M$  networks  $f_{\theta^k}$  where  $0 < k \leq M$ , whose
   weights are aggregated every  $\lambda$  epochs. Training
   Dataset for each network  $f_{\theta^k}$  is represented by  $D^k =$ 
    $\{(x_i^k, y_i^k)\}$ . The union of all datasets is denoted as  $D^*$ .
   Number of training epochs  $E$ , Maximum Learning Rate
    $LR_{max}$ , Cross-entropy loss  $\ell_{CE}$ . Model is trained using
   ERM for  $E'$  epochs initially.
2: for  $epoch = 1$  to  $E$  do
3:    $LR = 0.5 \cdot LR_{max} \cdot (1 + \cos((epoch - 1)/E \cdot \pi))$ 
4:   if  $epoch < E'$  then
5:      $\theta = \min_{\theta} \frac{1}{n} \sum_{i=1}^n \ell_{CE}(\theta, D^*)$ 
6:   else
7:     if  $epoch = E'$  then
8:        $\theta^k \leftarrow \theta \quad \forall k \in [1, M]$ 
9:     end if
10:     $\theta^k = \min_{\theta^k} \frac{1}{n} \sum_{i=1}^n \ell_{CE}(\theta, D^k) \quad \forall k \in [1, M]$ 
11:    if  $epoch \% \lambda = 0$  then
12:       $\theta = \frac{1}{M} \sum_{k=1}^M \theta^k$ 
13:       $\theta^k \leftarrow \theta \quad \forall k \in [1, M]$ 
14:    end if
15:  end if
16: end for

```

with a low loss barrier, when different permutations of their weights are considered, suggesting that *all solutions effectively lie in a common basin* [17]. Motivated by these observations (discussed in Section-2) and the above hypothesis, we aim at designing an algorithm that explores the basin of solutions effectively with a robust optimization path and combines the expertise of several diverse models to obtain a single generalized solution.

We show an outline of the proposed approach - *Diversify-Aggregate-Repeat Training*, dubbed DART, in Fig.1. Broadly, the proposed approach is implemented in four steps - i) ERM training for E' epochs in the beginning, followed by ii) Training M *Diverse* models for λ/M epochs each, iii) *Aggregating* their weights, and finally iv) *Repeating* the steps *Diversify-Aggregate* for $E - E'$ epochs.

A cosine learning rate schedule is used for training the model for a total of E epochs with a maximum learning rate of LR_{max} . We present the implementation of DART in Algorithm-1, and discuss each step in detail below:

1. **Traversing to the Basin of optimal solutions:** Since the goal of the proposed approach is to explore the *basin* of optimal solutions, the first step is to traverse from a randomly initialized model upto the periphery of this basin. Towards this, the proposed *Mixed-Training* strategy discussed in Section-1 is performed

on a combination of several augmentations D^* for the initial E' epochs (L4-L5 in Alg.1).

2. **Diversify - Exploring the Basin:** In this step, M diverse models f_{θ^k} initialized from the Mixed-Training model (L8 in Alg.1), are trained using the respective datasets D^k (L10 in Alg.1). These are generated using diverse augmentations in the In-Domain setting, and from a combination of different domains in the Domain Generalization setting. To maintain the same compute as baselines, we set $|D^k| = |D|/M$.
3. **Aggregate - Combining diverse experts:** Owing to the initial common training for E' epochs, the k diverse models lie in the same basin, enabling an effective aggregation of their weights using simple averaging (L12 in Alg.1) to obtain a more generalized solution θ . Aggregation is done after every λ epochs.
4. **Repeat:** Next, all k models are reinitialized using the common model θ (L13 of Alg.1), after which the individual models are trained for λ epochs on their respective datasets D^k as discussed in Step-2, and the process continues for a total of $E - E'$ epochs.

Visualizing the Optimization Trajectory: We compare the optimization trajectory of the proposed approach DART with independent training on the same augmentations in Fig.2 after a common training of $E' = 100$ epochs on Mixed augmentations. We note that the models explore more in the initial phase of training, and lesser thereafter, which is a result of the cosine learning rate schedule and gradient magnitudes. The exploration in the initial phase helps in increasing the diversity of models, thereby improving the robustness to spurious features (as shown in Proposition-3) leading to a better optimization trajectory, while the smaller steps towards the end help in retaining the flatter optima obtained after Aggregation. The process of repeated aggregation also ensures that the models remain close to each other, allowing longer training regimes.

5. Theoretical Results

We use the theoretical setup from Shen *et al.* [61] to show that the proposed approach DART achieves robustness to spurious features, thereby improving generalization.

Preliminaries and Setup: We consider a binary classification problem with two classes $\{-1, 1\}$. We assume that the dataset contains n inputs and K orthonormal robust features which are important for classification and are represented as $v_1, v_2, v_3, \dots, v_K$, in decreasing order of their frequency in the dataset. Let each input example x be composed of two patches denoted as $(x_1, x_2) \in R^{d \times 2}$, where each patch is characterized as follows: i) **Feature patch:** $x_1 = yv_{k^*}$ where y is the target label of x and $k^* \in [1, K]$, ii) **Noisy patch:** $x_2 = \epsilon$ where $\epsilon \sim \mathcal{N}\left(0, \frac{\sigma^2}{d} I_d\right)$.

We consider a single layer convolutional neural network consisting of C channels, with $w = (w_1, w_2, w_3, \dots, w_C) \in R^{d \times C}$. The function learned by the neural network (F) is given by $F(w, x) = \sum_{c=1}^C \sum_{p=1}^2 \phi(w_c, x_p)$, where ϕ is the activation function as defined by Shen *et al.* [61].

Weights learned by an ERM trained model: Let K_{cut} denote the number of robust features learned by the model. Following Shen *et al.* [61], we assume the learned weights to be a linear combination of the two types of features present in the dataset as shown below:

$$w = \sum_{k=1}^{K_{cut}} v_k + \sum_{k>K_{cut}} y^{(k)} \epsilon^{(k)} \quad (1)$$

Data Augmentations: As defined by Shen *et al.* [61], an augmentation T_k can be defined as follows:

$$\forall k' \in [1, K], \quad T_k(v_{k'}) = v_{((k'+k-1) \bmod K)+1} \quad (2)$$

Assuming that K unique augmentation strategies are used (where K denotes the number of robust patches in the dataset), augmented data is defined as follows:

$$D_{train}^{(aug)} = D_{train} \cup T_1(D_{train}) \cup \dots \cup T_{K-1}(D_{train}) \quad (3)$$

where D_{train} is the training dataset. This ensures that each feature patch v_i appears n times in the dataset, thus making the distribution of all the feature patches uniform.

Weight Averaging in DART: In the proposed method, we consider that m models are being independently trained after which their weights are averaged as shown below:

$$w = \frac{1}{m} \sum_{j=1}^m \sum_{k=1}^{K_{cut}} v_{k_j} + \frac{1}{m} \sum_{j=1}^m \sum_{k>K_{cut}} y_j^{(k)} \epsilon_j^{(k)} \quad (4)$$

Each branch is trained on the dataset $D_{train}^{(k)}$ defined as:

$$D_{train}^{(k)} = T_k(D_{train}), \quad k \in [1, m] \quad (5)$$

Propositions: In the following propositions, we derive the convergence time for learning robust and noisy features, and compare with the bounds derived by Shen *et al.* [61] in Section-6. The proofs of all propositions are presented in the Section-9.

Notation: Let f_θ denote a neural network obtained by averaging the weights of m individual models f_θ^k , $k \in [1, m]$ which are represented as shown in Eq.1. n is the total number of data samples present in the original dataset D_{train} . K is the number of orthonormal robust features present in the dataset. The weights w_1, w_2, \dots, w_C of each model f_θ^k are initialized as $w_c \sim \mathcal{N}(0, \sigma_0^2 I_d)$ $\forall c \in [1, C]$, where

C is the number of channels present in a single layer of the model. $\frac{\sigma}{\sqrt{d}}$ is the standard deviation of the noise present in noisy patches, q is a hyperparameter used to define the activation (Details in the Section-9), where $q \geq 3$ and d is the dimension of each feature patch and weight channel w_c .

Proposition 1. *The convergence time for learning any feature patch $v_i \forall i \in [1, K]$ in at least one channel $c \in C$ of the weight averaged model f_θ using the augmentations defined in Eq.5, is given by $O\left(\frac{K}{\sigma_0^{q-2}}\right)$, if $\frac{\sigma^q}{\sqrt{d}} \ll \frac{1}{K}$, $m = K$.*

Proposition 2. *If the noise patches learned by each f_θ^k are i.i.d. Gaussian random variables $\sim \mathcal{N}(0, \frac{\sigma^2}{d} I_d)$ then with high probability, convergence time of learning a noisy patch $\epsilon^{(j)}$ in at least one channels $c \in [1, C]$ of the weight averaged model f_θ is given by $O\left(\frac{nm}{\sigma_0^{q-2} \sigma^q}\right)$, if $d \gg n^2$.*

Proposition 3. *If the noise learned by each f_θ^k are i.i.d. Gaussian random variables $\sim \mathcal{N}(0, \frac{\sigma^2}{d} I_d)$, and model weight averaging is performed at epoch T , the convergence time of learning a noisy patch $\epsilon^{(j)}$ in at least one channels $c \in [1, C]$ of the weight averaged model f_θ is given by $T + O\left(\frac{nm^{(q-2)} d^{(q-2)/2}}{\sigma^{(2q-2)}}\right)$ if $d \gg n^2$.*

6. Analysis on the Theoretical Results

In this section, we present the implications of the theoretical results discussed above. While the setup in Section-5 discussed the existence of only two kinds of patches (feature and noisy), in practice, a combination of these two kinds of patches - termed as Spurious features - could also exist, whose convergence can be derived from the above results.

6.1. Learning Diverse Robust Features

We first show that *using sufficiently diverse data augmentations during training generates a uniform distribution of feature patches, encouraging the learning of diverse and robust features by the network*. We consider the use of K unique augmentations (where K is the number of robust patches in the dataset) in Eq.3 which transform each feature patch into a different one using a unique mapping as shown in Eq.2. The mapping in Eq.2 can transform a skewed feature distribution to a more uniform distribution after performing augmentations. This results in K_{cut} being sufficiently large in Eq.1, which depends on the number of high frequency robust features, thereby encouraging the learning of a more balanced distribution of robust features.

Shen *et al.* showed that the time to learn any feature patch v_k by at least one weight channel $c \in C$ is given by $O\left(\frac{1}{\sigma_0^{q-2} \rho_k}\right)$ if $\frac{\sigma^q}{\sqrt{d}} \ll \rho_k$, where ρ_k is the fraction of the frequency of occurrence of feature patch v_k divided by the total number of occurrences of all the feature patches in the dataset. The convergence time for learning feature patches

is thus limited by the one that is least frequent in the input data. Therefore, by making the frequency of occurrence of all feature patches uniform, the convergence time reduces. In Proposition-1, we show that the same holds true even for the proposed method DART where several branches are trained using diverse augmentations and their weights are finally averaged to obtain the final model. This justifies the improvements obtained in Mixed-Training (MT) (Eq.1) and in the proposed approach DART (Eq.4) as shown in Table-2.

6.2. Robustness to Noisy Features

Firstly, the use of diverse augmentations in both Mixed-Training (MT) and DART results in better robustness to noisy features since the value of K_{cut} in Eq.1 and Eq.4 would be higher, resulting in the learning of more feature patches and suppressing the learning of noisy patches. *The proposed method DART indeed suppresses the learning of noisy patches further, and also increases the convergence time for learning noisy features as shown in Proposition-2.* When the augmentations used in each of the m individual branches of DART are diverse, the noise learned by each of them can be assumed to be *i.i.d.* Under this assumption, averaging model weights at the end of training results in a reduction of noise variance, as shown in Eq.4. More formally, we show in Proposition-2 that the *convergence time of noisy patches increases by a factor of m when compared to ERM training.* We note that this does not hold in the case of averaging model weights obtained during a single optimization trajectory as in SWA [33], EMA or SWAD [6], since the noise learned by models that are close to each other in the optimization trajectory cannot be assumed to be *i.i.d.*

6.3. Impact of Intermediate Interpolations

We next analyse the impact of averaging the weights of the models at an intermediate epoch-T in addition to the interpolation at the end of training. The individual models are further reinitialized using the weights of the interpolated model as discussed in Algorithm-1. As shown in Proposition-3, averaging the weights of all branches at the intermediate epoch T helps in increasing the convergence time of noisy patches by a factor $O\left(\frac{\sigma_0^{q-2} m^{q-3} d^{(q-2)/2}}{\sigma^{q-2}}\right)$ when compared to the case where models are interpolated only at the end of training as shown in Proposition-2. By assuming that $q > 3$ and $d \gg n^2$ similar to Shen *et al.* [61], the lower bound on this can be written as $O\left(\frac{\sigma_0 n}{\sigma}\right)$. We note that in a practical scenario this factor would be greater than 1, demonstrating the increase in convergence time for noisy patches when intermediate interpolation is done.

7. Experiments and Results

In this section, we empirically demonstrate the performance gains obtained using the proposed approach DART on In-Domain (ID) and Domain Generalization

Table 2. **In-Domain Generalization:** Performance (%) of DART when compared to baselines on WideResNet-28-10 model. Standard deviation for DART and MT are reported across 5 reruns.

Method	CIFAR-10	CIFAR-100
ERM+EMA (Pad+Crop+HFlip)	96.41	81.67
ERM+EMA (AutoAugment)	97.50	84.20
ERM+EMA (Cutout)	97.43	82.33
ERM+EMA (Cutmix)	97.11	84.05
Learning Subspaces [74]	97.46	83.91
ERM+EMA (Mixed Training-MT)	97.69 ± 0.19	85.57 ± 0.13
DART (Ours)	97.96 ± 0.06	86.46 ± 0.12

(DG) datasets. We further attempt to understand the various factors that contribute to the success of DART.

Dataset Details: To demonstrate In-Domain generalization, we present results on CIFAR-10 and CIFAR-100 [38], while for Domain Generalization, we present results on the 5 real-world datasets on the DomainBed [24] benchmark - VLCS [18], PACS [42], OfficeHome [68], Terra Incognita [3] and DomainNet [51], which represent several types of domain shifts with different levels of dataset and task complexity. DomainNet is a large scale dataset with 6 domains, 345 categories and roughly 0.6 million images. More details on datasets are presented in Section-12.1.

Training Details (ID): We set the number of training epochs to 600 for the In-Domain experiments on CIFAR-10 and CIFAR-100. To enable a fair comparison, we select the best performing configuration amongst 200, 400 and 600 total training epochs for the ERM baselines and Mixed-Training, since they may be prone to overfitting. We use a cosine learning rate schedule with a maximum learning rate of 0.1 and weight decay of 5e-4. SGD with momentum of 0.9 is used for optimization of the cross-entropy (CE) loss. Interpolation frequency (λ) is set to be 50 epochs for CIFAR-100 and 40 epochs for CIFAR-10. We present results on ResNet-18 and WideResNet-28-10 architectures.

Training Details (DG): Following the setting in DomainBed [24], we use Adam [37] optimizer with a fixed learning rate of 5e-5. The number of training iterations are set to 15k for DomainNet (due to its higher complexity) and 10k for all other datasets with the interpolation frequency being set to 1k iterations. ResNet-50 [25] was used as the backbone, initialized with Imagenet [57] pre-trained weights. Best-model selection across training checkpoints was done based on validation results from the train domains itself, and no subset of the test domain was used. We present further details in Section-12.1.

SOTA comparison - In Domain (ID) Generalization: In Table-2, we compare our method against ERM training with several augmentations, and also the strong Mixed-Training benchmark (MT) obtained by using either AutoAugment [10], Cutout [12] or Cutmix [79] for every image in the training minibatch uniformly at random. We use

Table 3. **Domain Generalization:** OOD accuracy(%) of DART trained using ResNet50 compared to the respective baselines on DomainBed datasets. Standard dev. across 3 reruns is reported.

Algorithm	VLCS	PACS	OfficeHome	TerraInc	DomainNet	Avg
ERM [67]	77.5 \pm 0.4	85.5 \pm 0.2	66.5 \pm 0.3	46.1 \pm 1.8	40.9 \pm 0.1	63.3
+ DART (Ours)	78.5 \pm 0.7	87.3 \pm 0.5	70.1 \pm 0.2	48.7 \pm 0.8	45.8	66.1
SWAD [6]	79.1 \pm 0.1	88.1 \pm 0.1	70.6 \pm 0.2	50.0 \pm 0.3	46.5 \pm 0.1	66.9
+ DART (Ours)	80.3 \pm 0.2	88.9 \pm 0.1	71.9 \pm 0.1	51.3 \pm 0.2	47.2	67.9

Table 4. **Combining DART with other DG methods:** OOD performance (%) on OfficeHome (trained using ResNet50) of the proposed method DART coupled with different algorithms against their vanilla and SWAD counterparts. Numbers represented with \dagger were reproduced while others are from Domainbed.

Algorithm	Vanilla	DART (w/o SWAD)	SWAD	DART (+ SWAD)
ERM [67]	66.5	70.31	70.60	72.28
ARM [82]	64.8	69.24	69.75	71.31
SAM \dagger [19]	67.4	70.39	70.26	71.55
Cutmix \dagger [79]	67.3	70.07	71.08	71.49
Mixup [73]	68.1	71.14	71.15	72.38
DANN [21]	65.9	70.32	69.46	70.85
CDANN [44]	65.8	70.75	69.70	71.69
SagNet [48]	68.1	70.19	70.84	71.96

the same augmentations in DART as well, with each of the 3 branches being trained on one of the augmentations. As discussed in Section-3, the method proposed by Wortsman *et al.* [74] is closest to our approach, and hence we compare with it as well. We utilize Exponential Moving Averaging (EMA) of weights for the ERM baselines and the proposed approach for a fair comparison. On CIFAR-10, we observe gains of 0.19% on using ERM-EMA (Mixed) and an additional 0.27% on using DART. On CIFAR-100, 1.37% improvement is observed with ERM-EMA (Mixed) and an additional 0.89% with the proposed method DART. The comparison of DART with ERM on ImageNet-1K and fine-grained datasets like Stanford-Cars and CUB200 is shown in Table-6. On ImageNet-1K we observe gains of 0.41% on using RandAugment across all the branches of the model and of 0.14% on using Pad-Crop, RandAugment and Cutout for different branches. We observe gains upto 1.5% on fine-grained datasets.

SOTA comparison - Domain Generalization: We present results on the DomainBed [24] datasets in Table-3. We compare only with ERM training (performed on data from a mix of all domains) and SWAD [6] in the main paper due to lack of space, and present a thorough comparison across all other baselines in Table-12.3.1 in Appendix. For the DG experiments, we consider 4 branches ($M = 4$), with 3 branches being specialists on a given domain and the fourth being trained on a combination of all domains in equal proportion. For the DomainNet dataset, we consider 6 branches due to the presence of more domains. On average, we obtain 2.8% improvements over the ERM baseline without integrating with SWAD, and 1% higher accuracy when

Table 5. **DART using same augmentation across all branches:** Performance (%) of the DART when compared to baselines across different augmentations on CIFAR-100 using WideResNet-28-10 architecture. DART is better than baselines in all cases.

Method	Pad+Crop+HFlip	AutoAug.	Cutout	Cutmix	Mixed-Train.
ERM	81.48	83.93	82.01	83.02	85.54
ERM + EMA	81.67	84.20	82.33	84.05	85.57
DART (Ours)	82.31	85.02	84.15	84.72	86.13

compared to SWAD by integrating our approach with it. We further note from Table-4 that the DART can be integrated with several base approaches - with and without SWAD, while obtaining substantial gains across the respective baselines. The best performance achieved is by integrating with Mixup, which yields 3.04% better accuracy over ERM without SWAD, and 1.23% improvement over SWAD by integrating with it. The proposed approach therefore is generic, and can integrated effectively with several algorithms. As observed in Table-7, we observe substantial gains (+2.6%) over MIRO [7] on incorporating DART with SWAD and MIRO and using CLIP [55] as the backbone.

Evaluation without imposing diversity across branches: While the proposed method imposes diversity across branches by using different augmentations, we show in Table-5 that the method works even without explicitly introducing diversity, by virtue of the randomness introduced by SGD and different ordering of input samples across models. We obtain an average improvement of 0.9% over the respective baselines, and maximum improvement of 1.82% using Cutout. This shows that the performance of DART is not dependent on data augmentations, although it achieves further improvements on using them.

Table 6. **DART on ImageNet-1K and finegrained datasets:** Performance (%) of DART when compared to ERM on ResNet-50, when RandAugment [11] is used in all branches for ImageNet-1K and Pad-Crop for finegrained datasets (*Single Augmentation*) and when Pad-Crop, RandAugment [11] and Cutout [12] are used for different branches (*Mixed Augmentation*), while instead of RandAugment, AutoAugment is used for finegrained datasets.

Augmentation	Stanford-CARS (RN50, IN1k init.)		CUB200 (RN50, IN1k init.)		IN1k (RN50)	
	ERM	DART	ERM	DART	ERM	DART
Single Augmentation	88.11	90.42	78.55	79.75	78.55	78.96
Mixed Augmentation	90.88	91.95	81.72	82.83	79.06	79.20

Table 7. **Integrating DART with MIRO:** OOD performance (%) on OfficeHome of the proposed method DART coupled with MIRO [7] and SWAD [6] on different pretrained backbones.

Backbone	MIRO	MIRO+SWAD	DART	DART+MIRO	DART+MIRO+SWAD
ResNet-50 (IN-1k init.)	70.50	72.40	70.10	72.50	72.70
ViT-B16 (CLIP init.)	83.35	84.80	80.98	86.14	87.37

Accuracy across training epochs: We show the accuracy across training epochs for the individual branches and the combined model in Fig.4 for two cases - (a) performing

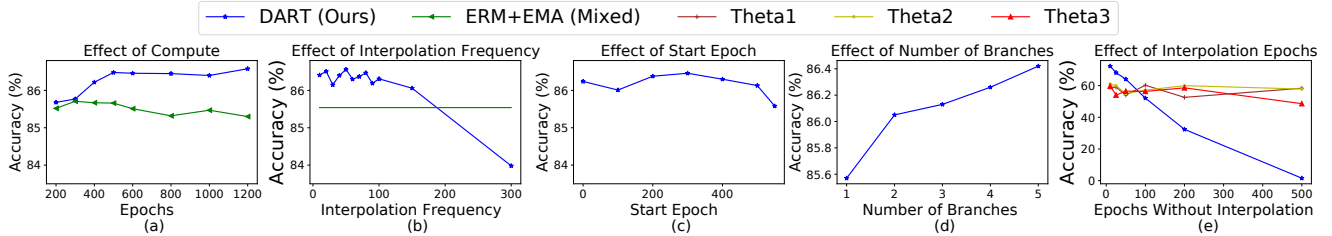


Figure 3. **Ablations on CIFAR-100, WideResNet-28-10:** (a-d) Experiments comparing DART with the Mixed-Training baseline using the standard training settings. (e) Varying the interpolation epoch after 50 epochs of common training using a fixed learning rate of 0.1.

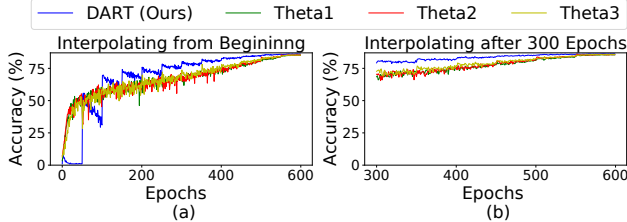


Figure 4. **Accuracy of DART across training epochs** for CIFAR-100 on WideResNet-28-10 model: Each branch is trained on different augmentations, whose accuracy is also plotted. Model Interpolation is done (a) from the beginning, (b) after 300 epochs. Although model interpolation and reinitialization happens every 50 epochs, interpolated model accuracy is plotted every epoch.

interpolations from the beginning, and (b) performing interpolations after half the training epochs, as done in DART. It can be noted from (a) that the interpolations in the initial few epochs have poor accuracy since the models are not in a common basin. Further, as seen in initial epochs of (a), when the learning rate is high, SGD training on an interpolated model cannot retain the flat solution due to its implicit bias of moving towards solutions that minimize train loss alone. Whereas, in the later epochs as seen in (b), the improvement obtained after every interpolation is retained. We therefore propose a common training strategy for the initial half of epochs, and split training after that.

Ablation experiments: We note the following observations from the plots in Fig.3 (a-e):

- (a) **Effect of Compute:** Using DART, we obtain higher (or similar) performance gains as the number of training epochs increases, whereas the accuracy of ERM+EMA (Mixed) baseline starts reducing after 300 epochs of training. This can be attributed to the increase in convergence time for learning noisy (or spurious) features due to the intermediate aggregations as shown in Proposition-3, which prevents overfitting.
- (b) **Effect of Interpolation Frequency:** We note that an optimal range of λ or the number of epochs between interpolations is 10 - 80, and we set this value to 50. If there is no interpolation for longer epochs, the models drift apart too much, causing a drop in accuracy.
- (c) **Effect of Start Epoch:** We note that although the proposed approach works well even if interpolations are

done from the beginning, by performing ERM training on mixed augmentations for 300 epochs, we obtain 0.22% improvement. Moreover, since interpolations do not help in the initial part of training as seen in Fig.4 (a), we propose to start this only in the second half.

- (d) **Effect of Number of branches:** As the number of branches increases, we note an improvement in performance due to higher diversity across branches, leading to more robustness to spurious features and better generalization as shown in Proposition-2.
- (e) **Effect of Interpolation epochs:** We perform a run with 50 epochs of common training followed by a single interpolation. We use a fixed learning rate and plot accuracy by varying the interpolation epoch. As this value increases, models drift far apart, reducing the accuracy after interpolation. At epoch-500, the accuracy even reaches 0, highlighting the importance of having a low loss barrier between models.

8. Conclusion

In this work, we first show that ERM training using a combination of *diverse* augmentations within a training minibatch can be a strong benchmark for ID generalization, which is only outperformed by ensembling the outputs of individual experts. Motivated by this observation, we present DART - Diversify-Aggregate-Repeat Training, to achieve the benefits of both training diverse experts and combining their expertise throughout training. The proposed algorithm first trains several models on different augmentations (or domains) to learn a *diverse* set of features, and further *aggregates* their weights to obtain better generalization. We repeat the steps Diversify-Aggregate several times over training, and show that this makes the optimization trajectory more robust by suppressing the learning of noisy features, while also ensuring a low loss barrier between the individual models to enable their effective aggregation. We justify our approach both theoretically and empirically on several benchmark In-Domain and Domain Generalization datasets, and show that it integrates effectively with several base training algorithms. We hope our work motivates further research on leveraging the linear mode connectivity of models for better generalization.

References

[1] Sravanti Addepalli, Samyak Jain, and R Venkatesh Babu. Efficient and effective augmentation strategy for adversarial training. *arXiv preprint arXiv:2210.15318*, 2022. 1

[2] Martin Arjovsky, Léon Bottou, Ishaaq Gulrajani, and David Lopez-Paz. Invariant risk minimization. *arXiv preprint arXiv:1907.02893*, 2019. 20

[3] Sara Beery, Grant Van Horn, and Pietro Perona. Recognition in terra incognita. In *Proceedings of the European conference on computer vision (ECCV)*, pages 456–473, 2018. 6

[4] Gilles Blanchard, Aniket Anand Deshmukh, Ürun Dogan, Gyemin Lee, and Clayton Scott. Domain generalization by marginal transfer learning. *The Journal of Machine Learning Research*, 22(1):46–100, 2021. 20

[5] Manh-Ha Bui, Toan Tran, Anh Tran, and Dinh Phung. Exploiting domain-specific features to enhance domain generalization. *Advances in Neural Information Processing Systems*, 34:21189–21201, 2021. 3

[6] Junbum Cha, Sanghyuk Chun, Kyungjae Lee, Han-Cheol Cho, Seunghyun Park, Yunsung Lee, and Sungrae Park. Swad: Domain generalization by seeking flat minima. *Advances in Neural Information Processing Systems*, 34:22405–22418, 2021. 1, 3, 6, 7, 18, 20

[7] Junbum Cha, Kyungjae Lee, Sungrae Park, and Sanghyuk Chun. Domain generalization by mutual-information regularization with pre-trained models. *European Conference on Computer Vision (ECCV)*, 2022. 7

[8] Prithvijit Chattopadhyay, Yogesh Balaji, and Judy Hoffman. Learning to balance specificity and invariance for in and out of domain generalization. In *European Conference on Computer Vision*, pages 301–318. Springer, 2020. 3

[9] Ching-Yao Chuang, Antonio Torralba, and Stefanie Jegelka. Estimating generalization under distribution shifts via domain-invariant representations. *arXiv preprint arXiv:2007.03511*, 2020. 2

[10] Ekin D Cubuk, Barret Zoph, Dandelion Mane, Vijay Vasudevan, and Quoc V Le. Autoaugment: Learning augmentation policies from data. *arXiv preprint arXiv:1805.09501*, 2018. 1, 2, 6

[11] Ekin D Cubuk, Barret Zoph, Jonathon Shlens, and Quoc V Le. Randaugment: Practical automated data augmentation with a reduced search space. In *Proceedings of the IEEE/CVF conference on computer vision and pattern recognition workshops*, pages 702–703, 2020. 1, 2, 7

[12] Terrance DeVries and Graham W Taylor. Improved regularization of convolutional neural networks with cutout. *arXiv preprint arXiv:1708.04552*, 2017. 1, 2, 6, 7

[13] Thomas G Dietterich. Ensemble methods in machine learning. In *International workshop on multiple classifier systems*, pages 1–15. Springer, 2000. 2

[14] Zhengming Ding and Yun Fu. Deep domain generalization with structured low-rank constraint. *IEEE Transactions on Image Processing*, 27(1):304–313, 2018. 3

[15] Felix Draxler, Kambis Veschgini, Manfred Salmhofer, and Fred Hamprecht. Essentially no barriers in neural network energy landscape. In *International conference on machine learning*, pages 1309–1318. PMLR, 2018. 2, 3

[16] Gintare Karolina Dziugaite and Daniel M Roy. Computing nonvacuous generalization bounds for deep (stochastic) neural networks with many more parameters than training data. *arXiv preprint arXiv:1703.11008*, 2017. 1, 3

[17] Rahim Entezari, Hanie Sedghi, Olga Saukh, and Behnam Neyshabur. The role of permutation invariance in linear mode connectivity of neural networks. *arXiv preprint arXiv:2110.06296*, 2021. 4

[18] Chen Fang, Ye Xu, and Daniel N. Rockmore. Unbiased metric learning: On the utilization of multiple datasets and web images for softening bias. In *2013 IEEE International Conference on Computer Vision*, pages 1657–1664, 2013. 6

[19] Pierre Foret, Ariel Kleiner, Hossein Mobahi, and Behnam Neyshabur. Sharpness-aware minimization for efficiently improving generalization. *arXiv preprint arXiv:2010.01412*, 2020. 1, 3, 7

[20] Jonathan Frankle, Gintare Karolina Dziugaite, Daniel Roy, and Michael Carbin. Linear mode connectivity and the lottery ticket hypothesis. In *International Conference on Machine Learning*, pages 3259–3269. PMLR, 2020. 2, 3

[21] Yaroslav Ganin, Evgeniya Ustinova, Hana Ajakan, Pascal Germain, Hugo Larochelle, François Laviolette, Mario Marchand, and Victor Lempitsky. Domain-adversarial training of neural networks. *The journal of machine learning research*, 17(1):2096–2030, 2016. 7, 18, 20

[22] Timur Garipov, Pavel Izmailov, Dmitrii Podoprikhin, Dmitry P Vetrov, and Andrew G Wilson. Loss surfaces, mode connectivity, and fast ensembling of dnns. *Advances in neural information processing systems*, 31, 2018. 2, 3

[23] Robert Geirhos, Patricia Rubisch, Claudio Michaelis, Matthias Bethge, Felix A Wichmann, and Wieland Brendel. Imagenet-trained cnns are biased towards texture; increasing shape bias improves accuracy and robustness. *arXiv preprint arXiv:1811.12231*, 2018. 1

[24] Ishaaq Gulrajani and David Lopez-Paz. In search of lost domain generalization. *arXiv preprint arXiv:2007.01434*, 2020. 1, 3, 6, 7, 19

[25] Kaiming He, Xiangyu Zhang, Shaoqing Ren, and Jian Sun. Deep residual learning for image recognition. In *2016 IEEE Conference on Computer Vision and Pattern Recognition (CVPR)*, pages 770–778, 2016. 6

[26] Dan Hendrycks and Thomas Dietterich. Benchmarking neural network robustness to common corruptions and perturbations. In *International Conference on Learning Representations*, 2019. 1, 20

[27] Dan Hendrycks*, Norman Mu*, Ekin Dogus Cubuk, Barret Zoph, Justin Gilmer, and Balaji Lakshminarayanan. Augmix: A simple method to improve robustness and uncertainty under data shift. In *International Conference on Learning Representations*, 2020. 2, 20

[28] Elad Hoffer, Tal Ben-Nun, Itay Hubara, Niv Giladi, Torsten Hoefer, and Daniel Soudry. Augment your batch: Improving generalization through instance repetition. In *2020 IEEE/CVF Conference on Computer Vision and Pattern Recognition (CVPR)*, pages 8126–8135, 2020. 1

[29] Shoubo Hu, Kun Zhang, Zhitang Chen, and Laiwan Chan. Domain generalization via multidomain discriminant analy-

sis. In *Uncertainty in Artificial Intelligence*, pages 292–302. PMLR, 2020. 2

[30] W Ronny Huang, Zeyad Ali Sami Emam, Micah Goldblum, Liam H Fowl, Justin K Terry, Furong Huang, and Tom Goldstein. Understanding generalization through visualizations. In *"I Can't Believe It's Not Better!" NeurIPS 2020 workshop*, 2020. 1, 3

[31] Zeyi Huang, Haohan Wang, Eric P Xing, and Dong Huang. Self-challenging improves cross-domain generalization. In *European Conference on Computer Vision*, pages 124–140. Springer, 2020. 20

[32] Maximilian Ilse, Jakub M Tomczak, Christos Louizos, and Max Welling. Diva: Domain invariant variational autoencoders. In *Medical Imaging with Deep Learning*, pages 322–348. PMLR, 2020. 2

[33] Pavel Izmailov, Dmitrii Podoprikhin, Timur Garipov, Dmitry Vetrov, and Andrew Gordon Wilson. Averaging weights leads to wider optima and better generalization. *arXiv preprint arXiv:1803.05407*, 2018. 2, 3, 6

[34] Yiding Jiang, Behnam Neyshabur, Hossein Mobahi, Dilip Krishnan, and Samy Bengio. Fantastic generalization measures and where to find them. *arXiv preprint arXiv:1912.02178*, 2019. 1, 3

[35] Nitish Shirish Keskar, Dheevatsa Mudigere, Jorge Nocedal, Mikhail Smelyanskiy, and Ping Tak Peter Tang. On large-batch training for deep learning: Generalization gap and sharp minima. *arXiv preprint arXiv:1609.04836*, 2016. 2

[36] Aditya Khosla, Tinghui Zhou, Tomasz Malisiewicz, Alexei A Efros, and Antonio Torralba. Undoing the damage of dataset bias. In *European Conference on Computer Vision*, pages 158–171. Springer, 2012. 3

[37] Diederik P Kingma and Jimmy Ba. Adam: A method for stochastic optimization. *arXiv preprint arXiv:1412.6980*, 2014. 6

[38] Alex Krizhevsky. Learning multiple layers of features from tiny images. <https://www.cs.toronto.edu/~kriz/learning-features-2009-TR.pdf>, 2009. 6

[39] David Krueger, Ethan Caballero, Joern-Henrik Jacobsen, Amy Zhang, Jonathan Binas, Dinghuai Zhang, Remi Le Priol, and Aaron Courville. Out-of-distribution generalization via risk extrapolation (rex). In *International Conference on Machine Learning*, pages 5815–5826. PMLR, 2021. 20

[40] Balaji Lakshminarayanan, Alexander Pritzel, and Charles Blundell. Simple and scalable predictive uncertainty estimation using deep ensembles. *Advances in neural information processing systems*, 30, 2017. 2

[41] Da Li, Yongxin Yang, Yi-Zhe Song, and Timothy Hospedales. Learning to generalize: Meta-learning for domain generalization. In *Proceedings of the AAAI conference on artificial intelligence*, 2018. 20

[42] Da Li, Yongxin Yang, Yi-Zhe Song, and Timothy M. Hospedales. Deeper, broader and artier domain generalization. In *Proceedings of the IEEE International Conference on Computer Vision (ICCV)*, Oct 2017. 2, 3, 6

[43] Haoliang Li, Sinno Jialin Pan, Shiqi Wang, and Alex C. Kot. Domain generalization with adversarial feature learning. In *2018 IEEE/CVF Conference on Computer Vision and Pattern Recognition*, pages 5400–5409, 2018. 20

[44] Ya Li, Mingming Gong, Xinmei Tian, Tongliang Liu, and Dacheng Tao. Domain generalization via conditional invariant representations. In *Proceedings of the AAAI conference on artificial intelligence*, 2018. 7, 18, 20

[45] Ya Li, Xinmei Tian, Mingming Gong, Yajing Liu, Tongliang Liu, Kun Zhang, and Dacheng Tao. Deep domain generalization via conditional invariant adversarial networks. In *Proceedings of the European Conference on Computer Vision (ECCV)*, September 2018. 1, 2

[46] Soon Hoe Lim, N Benjamin Erichson, Francisco Utrera, Winnie Xu, and Michael W Mahoney. Noisy feature mixup. *arXiv preprint arXiv:2110.02180*, 2021. 1, 2

[47] Massimiliano Mancini, Zeynep Akata, Elisa Ricci, and Barbara Caputo. Towards recognizing unseen categories in unseen domains. In *European Conference on Computer Vision*, pages 466–483. Springer, 2020. 3

[48] Hyeonseob Nam, HyunJae Lee, Jongchan Park, Wonjun Yoon, and Donggeun Yoo. Reducing domain gap by reducing style bias. In *Proceedings of the IEEE/CVF Conference on Computer Vision and Pattern Recognition*, pages 8690–8699, 2021. 7, 20

[49] Behnam Neyshabur, Srinadh Bhojanapalli, David McAllester, and Nati Srebro. Exploring generalization in deep learning. *Advances in neural information processing systems*, 30, 2017. 2

[50] Quynh Nguyen. On connected sublevel sets in deep learning. In *International conference on machine learning*, pages 4790–4799. PMLR, 2019. 2, 3

[51] Xingchao Peng, Qinxun Bai, Xide Xia, Zijun Huang, Kate Saenko, and Bo Wang. Moment matching for multi-source domain adaptation. In *Proceedings of the IEEE International Conference on Computer Vision*, pages 1406–1415, 2019. 6

[52] Henning Petzka, Michael Kamp, Linara Adilova, Cristian Sminchisescu, and Mario Boley. Relative flatness and generalization. *Advances in Neural Information Processing Systems*, 34:18420–18432, 2021. 1, 3

[53] Vihari Piratla, Praneeth Netrapalli, and Sunita Sarawagi. Efficient domain generalization via common-specific low-rank decomposition. In *International Conference on Machine Learning*, pages 7728–7738. PMLR, 2020. 3

[54] Fengchun Qiao, Long Zhao, and Xi Peng. Learning to learn single domain generalization. In *Proceedings of the IEEE/CVF Conference on Computer Vision and Pattern Recognition*, pages 12556–12565, 2020. 3

[55] Alec Radford, Jong Wook Kim, Chris Hallacy, Aditya Ramesh, Gabriel Goh, Sandhini Agarwal, Girish Sastry, Amanda Askell, Pamela Mishkin, Jack Clark, Gretchen Krueger, and Ilya Sutskever. Learning transferable visual models from natural language supervision. In *International Conference on Machine Learning*, 2021. 7

[56] Alexandre Ramé, Rémy Sun, and Matthieu Cord. Mixmo: Mixing multiple inputs for multiple outputs via deep subnetworks. In *Proceedings of the IEEE/CVF International Conference on Computer Vision*, pages 823–833, 2021. 1

[57] Olga Russakovsky, Jia Deng, Hao Su, Jonathan Krause, Sanjeev Satheesh, Sean Ma, Zhiheng Huang, Andrej Karpathy,

Aditya Khosla, Michael Bernstein, et al. Imagenet large scale visual recognition challenge. *International journal of computer vision*, 115(3):211–252, 2015. 6

[58] Shiori Sagawa, Pang Wei Koh, Tatsunori B Hashimoto, and Percy Liang. Distributionally robust neural networks for group shifts: On the importance of regularization for worst-case generalization. *arXiv preprint arXiv:1911.08731*, 2019. 20

[59] Harshay Shah, Kaustav Tamuly, Aditi Raghunathan, Prateek Jain, and Praneeth Netrapalli. The pitfalls of simplicity bias in neural networks. *Advances in Neural Information Processing Systems*, 33:9573–9585, 2020. 1

[60] Shiv Shankar, Vihari Piratla, Soumen Chakrabarti, Siddhartha Chaudhuri, Preethi Jyothi, and Sunita Sarawagi. Generalizing across domains via cross-gradient training. *arXiv preprint arXiv:1804.10745*, 2018. 3

[61] Ruqi Shen, Sébastien Bubeck, and Suriya Gunasekar. Data augmentation as feature manipulation: a story of desert cows and grass cows. *arXiv preprint arXiv:2203.01572*, 2022. 1, 4, 5, 6, 12, 13

[62] Yichun Shi, Xiang Yu, Kihyuk Sohn, Manmohan Chandraker, and Anil K Jain. Towards universal representation learning for deep face recognition. In *Proceedings of the IEEE/CVF Conference on Computer Vision and Pattern Recognition*, pages 6817–6826, 2020. 3

[63] Saurabh Singh, Derek Hoiem, and David Forsyth. Swapout: Learning an ensemble of deep architectures. In *Advances in Neural Information Processing Systems*, volume 29. Curran Associates, Inc., 2016. 2

[64] David Stutz, Matthias Hein, and Bernt Schiele. Relating adversarially robust generalization to flat minima. In *Proceedings of the IEEE/CVF International Conference on Computer Vision*, pages 7807–7817, 2021. 3, 17, 18

[65] Baochen Sun and Kate Saenko. Deep coral: Correlation alignment for deep domain adaptation. In *European conference on computer vision*, pages 443–450. Springer, 2016. 20

[66] Norman Tatro, Pin-Yu Chen, Payel Das, Igor Melnyk, Prasanna Sattigeri, and Rongjie Lai. Optimizing mode connectivity via neuron alignment. *Advances in Neural Information Processing Systems*, 33:15300–15311, 2020. 3

[67] Vladimir Vapnik. Statistical learning theory wiley. *New York*, 1998. 7, 20

[68] Hemanth Venkateswara, Jose Eusebio, Shayok Chakraborty, and Sethuraman Panchanathan. Deep hashing network for unsupervised domain adaptation. In *Proceedings of the IEEE conference on computer vision and pattern recognition*, pages 5018–5027, 2017. 6

[69] Vikas Verma, Alex Lamb, Christopher Beckham, Amir Najafi, Ioannis Mitliagkas, David Lopez-Paz, and Yoshua Bengio. Manifold mixup: Better representations by interpolating hidden states. In *International Conference on Machine Learning*, pages 6438–6447. PMLR, 2019. 2

[70] Riccardo Volpi and Vittorio Murino. Addressing model vulnerability to distributional shifts over image transformation sets. In *Proceedings of the IEEE/CVF International Conference on Computer Vision (ICCV)*, October 2019. 3

[71] Riccardo Volpi, Hongseok Namkoong, Ozan Sener, John C Duchi, Vittorio Murino, and Silvio Savarese. Generalizing to unseen domains via adversarial data augmentation. *Advances in neural information processing systems*, 31, 2018. 3

[72] Guoqing Wang, Hu Han, Shiguang Shan, and Xilin Chen. Cross-domain face presentation attack detection via multi-domain disentangled representation learning. In *Proceedings of the IEEE/CVF Conference on Computer Vision and Pattern Recognition*, 04 2020. 3

[73] Yufei Wang, Haoliang Li, and Alex C Kot. Heterogeneous domain generalization via domain mixup. In *ICASSP 2020-2020 IEEE International Conference on Acoustics, Speech and Signal Processing (ICASSP)*, pages 3622–3626. IEEE, 2020. 3, 7, 20

[74] Mitchell Wortsman, Maxwell C Horton, Carlos Guestrin, Ali Farhadi, and Mohammad Rastegari. Learning neural network subspaces. In *International Conference on Machine Learning*, pages 11217–11227. PMLR, 2021. 2, 3, 6, 7

[75] Mitchell Wortsman, Gabriel Ilharco, Samir Ya Gadre, Rebecca Roelofs, Raphael Gontijo-Lopes, Ari S Morcos, Hongseok Namkoong, Ali Farhadi, Yair Carmon, Simon Kornblith, et al. Model soups: averaging weights of multiple fine-tuned models improves accuracy without increasing inference time. In *International Conference on Machine Learning*, pages 23965–23998. PMLR, 2022. 2, 3, 18

[76] Kai Xiao, Logan Engstrom, Andrew Ilyas, and Aleksander Madry. Noise or signal: The role of image backgrounds in object recognition. *arXiv preprint arXiv:2006.09994*, 2020. 1

[77] Zhenlin Xu, Deyi Liu, Junlin Yang, Colin Raffel, and Marc Niethammer. Robust and generalizable visual representation learning via random convolutions. *arXiv preprint arXiv:2007.13003*, 2020. 3

[78] Xiangyu Yue, Yang Zhang, Sicheng Zhao, Alberto Sangiovanni-Vincentelli, Kurt Keutzer, and Boqing Gong. Domain randomization and pyramid consistency: Simulation-to-real generalization without accessing target domain data. In *Proceedings of the IEEE/CVF International Conference on Computer Vision (ICCV)*, October 2019. 3

[79] Sangdoo Yun, Dongyoon Han, Seong Joon Oh, Sanghyuk Chun, Junsuk Choe, and Youngjoon Yoo. Cutmix: Regularization strategy to train strong classifiers with localizable features. In *Proceedings of the IEEE/CVF international conference on computer vision*, pages 6023–6032, 2019. 1, 2, 6, 7

[80] Chiyuan Zhang, Samy Bengio, Moritz Hardt, Benjamin Recht, and Oriol Vinyals. Understanding deep learning (still) requires rethinking generalization. *Communications of the ACM*, 64(3):107–115, 2021. 2

[81] Hongyi Zhang, Moustapha Cisse, Yann N Dauphin, and David Lopez-Paz. mixup: Beyond empirical risk minimization. *arXiv preprint arXiv:1710.09412*, 2017. 1, 2

[82] Marvin Zhang, Henrik Marklund, Nikita Dhawan, Abhishek Gupta, Sergey Levine, and Chelsea Finn. Adaptive risk minimization: Learning to adapt to domain shift. *Advances in Neural Information Processing Systems*, 34:23664–23678, 2021. 7, 20

[83] Shaofeng Zhang, Meng Liu, and Junchi Yan. The diversified ensemble neural network. *Advances in Neural Information Processing Systems*, 33:16001–16011, 2020. 2

[84] Pu Zhao, Pin-Yu Chen, Payel Das, Karthikeyan Natesan Ramamurthy, and Xue Lin. Bridging mode connectivity in loss landscapes and adversarial robustness. *arXiv preprint arXiv:2005.00060*, 2020. 3

[85] Kaiyang Zhou, Yongxin Yang, Timothy Hospedales, and Tao Xiang. Learning to generate novel domains for domain generalization. In *European conference on computer vision*, pages 561–578. Springer, 2020. 3

[86] Kaiyang Zhou, Yongxin Yang, Yu Qiao, and Tao Xiang. Domain generalization with mixstyle. *arXiv preprint arXiv:2104.02008*, 2021. 3

9. Theoretical Results

In this section, we present details on the theoretical results discussed in Section-5. As noted by Shen *et al.* [61], the weights learned by a patch-wise Convolutional Neural Network are a linear combination of the two types of features (described in Section-5 of the main paper) present in the dataset. Let the threshold K_{cut} denote the number of robust features learned by the model. We have,

$$w = \sum_{k \leq K_{cut}} v_k + \sum_{k > K_{cut}} y^{(k)} \epsilon^{(k)} \quad (6)$$

On averaging of the weights of m models we get:

$$w = \frac{1}{m} \sum_{j=1}^m \left[\sum_{k=1}^{K_{cut_j}} v_{k_j} + \sum_{k > K_{cut_j}} y_j^{(k)} \epsilon_j^{(k)} \right] \quad (7)$$

We now analyze the convergence of this weight averaged neural network shown in Eq.7. Let L represent the logistic loss of the model, F denote the function learned by the neural network, and w_c denote its weights across C channels indexed using c . Further, let $y^{(i)}$ represent the ground truth label of sample $x_i \forall i \in [1, n]$, where n denotes the number of samples in the train set. The weights w_1, w_2, \dots, w_C are initialized as $w_c \sim \mathcal{N}(0, \sigma_0^2 I_d) \forall c \in C$. We assume that the weights learned by the model at any time stamp t are a linear combination of the linear functions f, g and h corresponding to feature patches, noisy patches and model initialization respectively as shown below:

$$w_c^t = f(v_1, v_2, \dots, v_K) + g(\epsilon^{(1)}, \epsilon^{(2)}, \dots, \epsilon^{(n)}) + h(\epsilon') \quad (8)$$

where ϵ' is the random noise sampled for the initialization of the model. Since the term $h(\epsilon')$ does not play a role in the convergence of the model, we ignore this term for the purpose of analysis. For simplicity, we assume that f and g represent summations over their respective arguments. Thus, the weights at any time t can be represented as,

$$w_c^t = \sum_{l=1}^K \alpha_l^t v_l + \sum_{l > K_{cut}^t} y^{(l)} \epsilon^{(l)} \quad (9)$$

where K_{cut}^t and α_l^t are a functions of time t . At convergence, $\alpha_i = 1 \forall i \in [1, K_{cut}]$ and $\alpha_i = 0$ otherwise.

We now analyze the learning dynamics while training the model. Owing to the gradient descent based updates of model weights over time, the derivative of overall loss L w.r.t. the weights of a given channel w_c can be written as,

$$\begin{aligned} \frac{d}{dt} w_c &= -\frac{d}{dw_c} L \\ &= -\frac{1}{n} \sum_{i=1}^n y^{(i)} L'(y^{(i)} F(w, x^{(i)})) \nabla_{w_c} F(w, x^{(i)}) \end{aligned} \quad (10)$$

Since L is a logistic loss, we have $-L'(o(1)) = 0.5 + o(1)$, where $o(1)$ represents terms independent of the variable w . As discussed in Section-5 of the main paper, the function learned by the neural network is given by $F(w, x) = \sum_{c=1}^C \sum_{p=1}^2 \phi(w_c, x_p)$, where ϕ is the activation function defined as follows [61]:

- for $|z| \leq 1$; $\phi(z) = \text{sign}(z) \frac{1}{q} |z|^q$
- for $z \geq 1$; $\phi(z) = z - \frac{q-1}{q}$
- for $z \leq -1$; $\phi(z) = z + \frac{q-1}{q}$

Based on this, Eq.10 can be written as,

$$\frac{d}{dt} w_c \approx \frac{1 + o(1)}{2n} \sum_{i=1}^n \sum_{p=1}^2 \phi'(|w_c x_p^{(i)}|) y^{(i)} x_p^{(i)} \quad (11)$$

Considering the two types of patches present in the image (feature patches and noisy patches), we have:

$$\begin{aligned} \frac{d}{dt} w_c &\approx \frac{1 + o(1)}{2n} \sum_{i=1}^n \phi'(|w_c v_{d(i)}|) v_{d(i)} \\ &\quad + \frac{1 + o(1)}{2n} \sum_{i=1}^n \phi'(|w_c \epsilon^{(i)}|) y^{(i)} \epsilon^{(i)} \end{aligned} \quad (12)$$

where $v_{d(i)}$ represents the feature patch in the image $x^{(i)}$, $\frac{1+o(1)}{2n} \sum_{i=1}^n \phi'(|w_c v_{d(i)}|) v_{d(i)}$ represents the gradients on feature patches, and $\frac{1+o(1)}{2n} \sum_{i=1}^n \phi'(|w_c \epsilon^{(i)}|) y^{(i)} \epsilon^{(i)}$ represents the gradients on noisy patches of the image.

To improve the clarity of the proofs, we propose lemma-9 and lemma-9.

Lemma 1 *Let $X \sim N(0, \sigma_x^2 I_m)$ and $Y \sim N(0, \sigma_y^2 I_m)$ be N dimensional gaussian random variables, then $X^T Y = O(\sqrt{m} \sigma_x \sigma_y)$*

Proof. Given any two random variables $x \sim N(\mu_1, \sigma_1^2)$ and $y \sim N(\mu_2, \sigma_2^2)$

$$\begin{aligned} \text{Var}(xy) &= E[x^2y^2] - E[(xy)]^2 = \\ &= \text{Var}(x)\text{Var}(y) + \text{Var}(x)E(y)^2 + \text{Var}(y)E(x)^2 \\ &= \sigma_1^2\sigma_2^2 + \sigma_1^2\mu_2^2 + \sigma_2^2\mu_1^2 \quad (13) \end{aligned}$$

For $\mu_1 = \mu_2 = 0$, we get

$$\text{Var}(xy) = \text{Var}(x)\text{Var}(y) \quad (14)$$

Let $X \sim N(0, \sigma_x^2 I_m)$ and $Y \sim N(0, \sigma_y^2 I_m)$ be N dimensional gaussian random variables. It is same as, $X = [x_0, x_1, x_2, \dots, x_{m-1}]$ and $Y = [y_0, y_1, y_2, \dots, y_{m-1}]$, where $x_i \sim N(0, \sigma_x^2)$ and $y_i \sim N(0, \sigma_y^2) \forall i \in \{0, 1, 2, \dots, m-1\}$. We will first calculate $\text{Var}(X^T Y)$.

$$\text{Var}(X^T Y) = E[(X^T Y)^2] = E\left[\left(\sum_{i=0}^{m-1} x_i y_i\right)^2\right] \quad (15)$$

Since each x_i and y_i are sampled *iid* from a Gaussian with a fixed mean and variance, therefore $x_i y_i$ are *iid* random variables from the difference of two chi-squared distributions. The sum of k chi-squared random variables with mean μ and variance σ^2 , gives chi-squared distribution with mean $k\mu$ and variance $k\sigma^2$. Let $z = X^T Y$. Therefore by eq-14 z has mean 0 and variance $m\sigma_x^2\sigma_y^2$. Thus we have,

$$\text{Var}(z) = E(z^2) = m\sigma_x^2\sigma_y^2 \quad (16)$$

Using chebyshev's inequality, we have

$$P(|z| \geq k\sqrt{m}\sigma_x\sigma_y) \leq \frac{1}{k^2} \quad (17)$$

where k is some constant. Therefore we have

$$z = O(\sqrt{m}\sigma_x\sigma_y) \quad (18)$$

Further, by central limit theorem, we have the distribution $z = X^T Y = \sum_{i=0}^{m-1} x_i y_i$ is approximately Gaussian. Therefore, even for a smaller value of k , we can get a high confidence interval for bounding $|z|$. \square

Lemma 2 *Let V be a standard basis vector and $Y \sim N(0, \sigma_y^2 I_m)$ be N dimensional gaussian random variable, then $V^T Y = O(\sigma_y)$*

Proof. Let $z = v^T Y$. Let $Y \sim N(0, \sigma_y^2 I_m)$ be N dimensional gaussian random variable. Thus we have $V = [v_0, v_1, v_2, \dots, v_{m-1}]$ and $Y = [y_0, y_1, y_2, \dots, y_{m-1}]$, where

$y_i \sim N(0, \sigma_y^2) \forall i \in \{0, 1, 2, m-1\}$. Since V is a standard basis vector, we have

$$\begin{aligned} \text{Var}(z) &= E[(V^T Y)^2] = E\left[\left(\sum_{i=0}^{m-1} v_i y_i\right)^2\right] = \\ &= E[(y_k)^2] = \text{Var}(y_k) = \sigma_y^2 \quad (19) \end{aligned}$$

where k is some index for which $v_k = 1$ and $v_j = 0 \forall j \neq k$. Using chebyshev's inequality, we have

$$P(|z| \geq k\sigma_y) \leq \frac{1}{k^2} \quad (20)$$

where k is some constant. Therefore we have

$$z = O(\sigma_y) \quad (21)$$

\square

Based on lemma-9 and lemma-9, considering the weights $w_c \sim (0, \sigma_0^2 I_d)$, we have

$$|w_c v_k| = O(\sigma_0) \quad (22)$$

$$|w_c \epsilon^{(i)}| = O(\sigma \sigma_0) \quad (23)$$

$$|\epsilon^{(j)} \epsilon^{(i)}| = O\left(\frac{\sigma^2}{\sqrt{d}}\right) \quad (24)$$

$$|\epsilon^{(i)} v_k| = O\left(\frac{\sigma}{\sqrt{d}}\right) \quad (25)$$

9.1. Convergence time for feature patches

Proposition 1 *The convergence time for learning any feature patch $v_i \forall i \in [1, K]$ in at least one channel $c \in C$ of the weight averaged model f_θ using the augmentations defined in Eq.5, is given by $O\left(\frac{K}{\sigma_0^{q-2}}\right)$, if $\frac{\sigma^q}{\sqrt{d}} \ll \frac{1}{K}$, $m = K$.*

Proof. We first compute the convergence time without weight-averaging, as shown by Shen *et al.* [61]. The dot product between Eq.12 and any given feature v_k is given by:

$$\begin{aligned} \frac{d}{dt} w_c v_k &\approx \frac{1 + o(1)}{2} \rho_k \phi'(|w_c v_k|) \\ &\quad + \frac{1 + o(1)}{2n} \sum_{i=1}^n \phi'(|w_c \epsilon^{(i)}|) y^{(i)} \epsilon^{(i)} v_k \quad (26) \end{aligned}$$

where, ρ_k represents the fraction of v_k in the dataset. In eq-26 we can ignore $\frac{1+o(1)}{2n} \sum_{i=1}^n \phi'(|w_c \epsilon^{(i)}|) y^{(i)} \epsilon^{(i)} v_k$ as compared to $\frac{1+o(1)}{2n} \phi'(|w_c v_k|)$, if their values are of different orders at initialization. Since at initialization $w_c \sim (0, \sigma_0^2 I_d)$, using conditions listed in eq-22, 25 and 23, at initialization and using the definition of the activation function defined

for the case of $|w_c v_{d^{(i)}}| < 1$ and $|w_c \epsilon^{(i)}| < 1 \forall i \in [1, n]$, we get

$$\frac{1+o(1)}{2n} \phi'(|w_c v_k|) = O(\rho_k \sigma_0^{q-1}) \quad (27)$$

$$\frac{1+o(1)}{2n} \sum_{i=1}^n \phi'(|w_c \epsilon^{(i)}|) y^{(i)} \epsilon^{(i)} v_k = O\left(\frac{\sigma_0^{q-1} \sigma^q}{\sqrt{d}}\right) \quad (28)$$

Comparing eq-27 and eq-28, we get for If $\frac{\sigma^q}{\sqrt{d}} \ll \frac{1}{K}$, we can ignore $\frac{1+o(1)}{2n} \sum_{i=1}^n \phi'(|w_c \epsilon^{(i)}|) y^{(i)} \epsilon^{(i)} v_k$ as compared to $\frac{1+o(1)}{2n} \phi'(|w_c v_k|)$. This gives:

$$\frac{d}{dt}(w_c v_k) \approx \frac{1+o(1)}{2} \rho_k \phi'(|w_c v_k|) \quad (29)$$

We denote $w_c v_k$ at a time step t using a generic function $g(w_c, v_k, t)$. Using the definition of activation function ϕ as discussed above, and assuming that $|w_c v_k| < 1$ we get,

$$\frac{d(g(w_c, v_k, t))}{dt} = \frac{1+o(1)}{2} \rho_k g(w_c, v_k, t)^{q-1} \quad (30)$$

On integrating we get,

$$\begin{aligned} \frac{(1+o(1))\rho_k}{2} t - (q-2)(g(w_c, v_k, t=0)^{2-q} \\ = (2-q)(g(w_c, v_k, t=t)^{2-q}) \end{aligned} \quad (31)$$

For the term $g(w_c, v_d, t=t)^{2-q}$ to become $o(1)$ at the time of convergence, $\frac{(1+o(1))\rho_k}{2} t - (q-2)g(w_c, v_d, t=0)^{2-q}$ should be constant. Using eq-22, $t=0$, $g(w_c, v_d, t=0)^{2-q} = \sigma_0^{2-q}$, where σ_0 is the standard deviation of the zero-mean Gaussian distribution that is used for initializing the weights of the model. Thus, the convergence time to learn v_k by at least one channel $c \in C$, is given by:

$$t = O\left(\frac{1}{\rho_k \sigma_0^{q-2}}\right) \quad (32)$$

We now compute the convergence of the case where m models are averaged. We denote the averaged weights of a given channel c by w_c^{avg} . By substituting for w_c from Eq.9 we get,

$$\begin{aligned} -\frac{1}{m} \sum_{j=1}^m \frac{dL_j}{(d_{w_c})_j} v_k &= \frac{d(w_c^{avg})}{dt} v_k \\ &= \frac{1}{m} \sum_{j=1}^m \frac{d\left(\sum_{l=1}^K \alpha_{lj}^t v_l + \sum_{l>K_{cut}^t} y_j^{(l)} \epsilon_j^{(l)}\right) v_k}{dt} \end{aligned} \quad (33)$$

We note that from eq-25, $\sum_{l>K_{cut}^t} y_j^{(l)} \epsilon_j^{(l)} v_k = O\left(\frac{\sigma}{\sqrt{d}}\right)$.

Whereas $\sum_{l=1}^K \alpha_{lj}^t v_l = O(1)$ Thus we can ignore

$\sum_{l>K_{cut}^t} y_j^{(l)} \epsilon_j^{(l)} v_k$. Thus, we get

$$\frac{d(w_c^{avg})}{dt} v_k \approx \frac{1}{m} \frac{d\left(\sum_{j=1}^m \alpha_{kj}^t\right)}{dt} \quad (34)$$

A similar analysis for a single model that is not weight-averaged gives,

$$\frac{d(w_c)}{dt} v_k \approx \frac{d(\alpha_k^t)}{dt} = \frac{d(w_c^{avg})}{dt} v_k \frac{d(m\alpha_k^t)}{d\left(\sum_{j=1}^m \alpha_{kj}^t\right)} \quad (35)$$

As discussed in Section-5 of the main paper, we set $m = K$. Further, since the most frequent patches are learned faster, we assume that the relative rate of change in α_{kj} will depend on the relative frequency of individual patch features. Therefore, $\frac{d(\alpha_k^t)/dt}{d\left(\sum_{j=1}^m \alpha_{kj}^t\right)/dt} = \frac{d(\alpha_k^t)/dt}{d\left(\sum_{j=1}^K \alpha_{kj}^t\right)/dt} = \rho_k$. Thus we get,

$$\frac{d(w_c^{avg})}{dt} v_k = \frac{1}{\rho_k K} \frac{d(w_c)}{dt} v_k \quad (36)$$

In eq-36, we have the rate of change of $w_c^{avg} = \frac{1}{\rho_k K}$ times the rate of change of w_c . Therefore the time for convergence for w_c^{avg} will be $\rho_k K$ times the time for convergence for w_c , which gives

$$t = O\left(\frac{K}{\sigma_0^{q-2}}\right) \quad (37)$$

□

Corollary 1.1 *The convergence time for learning any feature patch $v_i \forall i \in [1, K]$ in at least one channel $c \in C$ of the weight averaged model f_θ using the augmentations defined in Eq.5, is given by $O\left(\frac{m\rho'_k}{\rho_k \sigma_0^{q-2}}\right)$, if $\frac{\sigma^q}{\sqrt{d}} \ll \frac{1}{K}$.*

Here ρ_k is the ratio between the frequency of the feature patch k in the dataset and the sum of the frequencies of all feature patches in the dataset. ρ'_k is the ratio between the frequency of the feature patch k in the dataset and the sum of the frequencies of some m feature patches $[v_{(k) \bmod K+1}, v_{(k+1) \bmod K+1}, \dots, v_{(m+k-1) \bmod K+1}]$

Proof. Since the most frequent patches are learned faster, we assume that the relative rate of change in α_{kj} will depend on the relative frequency of individual patch features. Therefore,

$$\frac{d(\alpha_k^t)/dt}{d\left(\sum_{j=1}^m \alpha_{kj}^t\right)/dt} = \frac{(\alpha_k^t)/dt}{\left(\sum_{j=1}^m \alpha_{kj}^t\right)/dt} = \rho'_k \quad (38)$$

Thus substituting in eq-35, we get

$$\frac{d(w_c^{avg})}{dt} v_k = \frac{1}{\rho'_k m} \frac{d(w_c)}{dt} v_k \quad (39)$$

In eq-39, we have the rate of change of $w_c^{avg} = \frac{1}{\rho_k K}$ times the rate of change of w_c . Therefore the time for convergence for w_c^{avg} will be $\rho_k m$ times the time for convergence for w_c , which gives

$$t = O\left(\frac{m\rho_k'}{\rho_k\sigma_0^{q-2}}\right) \quad (40)$$

□

The convergence time from prop-9.1 (denoted as t) can be written as

$$t = O\left(\frac{m \sum_{j=1}^K \alpha_{kj}}{\sum_{j=1}^m \alpha_{kj} \sigma_0^{q-2}}\right) \quad (41)$$

The convergence time from eq-32 (denoted as t') can be written as

$$t' = O\left(\frac{\sum_{j=1}^K \alpha_{kj}}{\alpha_k \sigma_0^{q-2}}\right) \quad (42)$$

For hard to learn feature patches (feature patches with low α_k), comparing eq-41 and eq-42, we observe that the convergence time will be higher in eq-42. Since a summation over some m feature patches is appearing in eq-41, therefore its convergence time has a lower impact on the frequency of an individual feature patch. This helps in increased learning of hard features, thereby improving generalization.

9.2. Convergence time of noisy patches

We consider the dot product between any noisy patch ϵ^k and Eq.12:

$$\begin{aligned} \frac{d}{dt} w_c \epsilon^{(k)} &= \frac{1+o(1)}{2n} \sum_{i=1}^n \phi'(|w_c v_{d^{(i)}}|) v_{d^{(i)}} \epsilon^{(k)} + \\ &\quad \frac{1+o(1)}{2n} \sum_{i=1}^n \phi'(|w_c \epsilon^{(i)}|) y^{(i)} \epsilon^{(i)} \epsilon^{(k)} \end{aligned} \quad (43)$$

On simplifying we get,

$$\begin{aligned} \frac{d}{dt} w_c \epsilon^{(k)} &= \frac{1+o(1)}{2n} \sum_{i=1}^n \phi'(|w_c v_{d^{(i)}}|) v_{d^{(i)}} \epsilon^{(k)} + \\ &\quad \frac{1+o(1)}{2n} \phi'(|w_c \epsilon^{(k)}|) y^{(k)} \|\epsilon^{(k)}\|^2 \\ &\quad + \frac{1+o(1)}{2n} \sum_{i=1; i \neq k}^n \phi'(|w_c \epsilon^{(i)}|) y^{(i)} \epsilon^{(i)} \epsilon^{(k)} \end{aligned} \quad (44)$$

In eq-44 we can ignore $\frac{1+o(1)}{2n} \sum_{i=1}^n \phi'(|w_c v_{d^{(i)}}|) v_{d^{(i)}} \epsilon^{(k)}$ + $\frac{1+o(1)}{2n} \sum_{i=1; i \neq k}^n \phi'(|w_c \epsilon^{(i)}|) y^{(i)} \epsilon^{(i)} \epsilon^{(k)}$ as compared to $\frac{1+o(1)}{2n} \phi'(|w_c \epsilon^{(k)}|) y^{(k)} \|\epsilon^{(k)}\|^2$, if their values are of different orders at initialization. Since at initialization $w_c \sim (0, \sigma_0^2 I_d)$, using conditions listed in eq-22, 24, 25 and 23, at initialization and using the definition of the activation function defined for the case of $|w_c v_{d^{(i)}}| < 1$ and $|w_c \epsilon^{(i)}| < 1 \forall i \in [1, n]$, we get

$$\frac{1+o(1)}{2n} \sum_{i=1}^n \phi'(|w_c v_{d^{(i)}}|) v_{d^{(i)}} \epsilon^{(k)} = O\left(\frac{\sigma_0^{q-1} \sigma}{\sqrt{d}}\right) \quad (45)$$

$$\frac{1+o(1)}{2n} \sum_{i=1; i \neq k}^n \phi'(|w_c \epsilon^{(i)}|) y^{(i)} \epsilon^{(i)} \epsilon^{(k)} = O\left(\frac{\sigma_0^{q-1} \sigma^{q+1}}{\sqrt{d}}\right) \quad (46)$$

Therefore

$$\begin{aligned} &\frac{1+o(1)}{2n} \sum_{i=1}^n \phi'(|w_c v_{d^{(i)}}|) v_{d^{(i)}} \epsilon^{(k)} + \\ &\frac{1+o(1)}{2n} \sum_{i=1; i \neq k}^n \phi'(|w_c \epsilon^{(i)}|) y^{(i)} \epsilon^{(i)} \epsilon^{(k)} = \\ &O\left(\frac{\sigma_0^{q-1} \sigma^{q+1}}{\sqrt{d}}\right) + O\left(\frac{\sigma_0^{q-1} \sigma}{\sqrt{d}}\right) \end{aligned} \quad (47)$$

$$\begin{aligned} &\frac{1+o(1)}{2n} \phi'(|w_c \epsilon^{(k)}|) y^{(k)} \|\epsilon^{(k)}\|^2 = \\ &\frac{1+o(1)}{2n} \sigma^2 \phi'(|w_c \epsilon^{(k)}|) y^{(k)} = O\left(\frac{\sigma^{q+1} \sigma_0^{q-1}}{n}\right) \end{aligned} \quad (48)$$

Comparing eq-48 and eq-47, we get if $d >> n^2$, we can ignore $\frac{1+o(1)}{2n} \sum_{i=1}^n \phi'(|w_c v_{d^{(i)}}|) v_{d^{(i)}} \epsilon^{(k)} + \frac{1+o(1)}{2n} \sum_{i=1; i \neq k}^n \phi'(|w_c \epsilon^{(i)}|) y^{(i)} \epsilon^{(i)} \epsilon^{(k)}$ as compared to $\frac{1+o(1)}{2n} \phi'(|w_c \epsilon^{(k)}|) y^{(k)} \|\epsilon^{(k)}\|^2$ Thus we get:

Using the activation defined earlier, and considering $w_c \epsilon^{(k)}$ as a generic function $g(w_c, \epsilon^{(k)}, t)$ at time stamp t , where $|g(w_c, \epsilon^{(k)}, t)| < 1$, we get,

$$\frac{d(g(w_c, \epsilon^{(k)}, t))}{dt} = \frac{1+o(1)}{2n} \sigma^2 g(w_c, \epsilon^{(k)}, t)^{q-1} \quad (49)$$

Similar to the analysis presented in Eq.31, on integrating the above equation we get,

$$\begin{aligned} &\frac{1+o(1)}{2n} t \sigma^2 - (q-2)(g(w_c, \epsilon^{(k)}, t=0)^{2-q} = \\ &\quad (2-q)(g(w_c, \epsilon^{(k)}, t=t)^{2-q}) \end{aligned} \quad (50)$$

Using eq-23, at $t = 0$,

$$g(w_c, \epsilon^{(k)}, t = 0)^{2-q} = \sigma_0^{2-q} \sigma^{2-q} \quad (51)$$

where σ_0 is the standard deviation of the zero-mean Gaussian distribution that is used for initializing the weights of the model, and $\frac{\sigma}{\sqrt{d}}$ is the standard deviation of the noise present in noisy patches. Thus we get,

$$\begin{aligned} \frac{1+o(1)}{2n} t \sigma^2 - (q-2) \sigma_0^{2-q} \sigma^{2-q} = \\ (2-q)(g(w_c, \epsilon^{(k)}, t = t)^{2-q}) \end{aligned} \quad (52)$$

For the term $g(w_c, \epsilon^{(k)}, t = t)^{2-q}$ to become $o(1)$ at the time of convergence, $\frac{1+o(1)}{2n} t \sigma^2 - (q-2) \sigma_0^{2-q} \sigma^{2-q}$ should be constant. Equating the L.H.S. of the above equation to 0, the convergence time to learn $\epsilon^{(k)}$ by at least one channel $c \in C$, is given by:

$$t = O\left(\frac{n}{\sigma_0^{q-2} \sigma^q}\right) \quad (53)$$

Proposition 2 If the noise patches learned by each f_θ^k are i.i.d. Gaussian random variables $\sim \mathcal{N}(0, \frac{\sigma^2}{d} I_d)$ then with high probability, convergence time of learning a noisy patch $\epsilon^{(j)}$ in at least one channel $c \in [1, C]$ of the weight averaged model f_θ is given by $O\left(\frac{nm}{\sigma_0^{q-2} \sigma^q}\right)$, if $d \gg n^2$.

Proof. By averaging the weights of m models in Eq.43 we get,

$$\begin{aligned} -\frac{1}{m} \sum_{j=1}^m \frac{dL_j}{(d_{w_e})_j} \epsilon^{(k)} = \frac{d(w_{avg})}{dt} \epsilon^{(k)} = \\ \frac{1}{m} \sum_{j=1}^m \left[\frac{1+o(1)}{2n} \sum_{i=1}^n \phi'(|w_{c_j} v_{d^{(i)}}|) v_{d^{(i)}} \epsilon^{(k)} + \right. \\ \left. \frac{1+o(1)}{2n} \sum_{i=1}^n \phi'(|w_{c_j} \epsilon^{(i)}|) y^{(i)} \epsilon^{(i)} \epsilon^{(k)} \right] \end{aligned} \quad (54)$$

$$\begin{aligned} = \frac{1}{m} \sum_{j=1}^m \left[\frac{1+o(1)}{2n} \sum_{i=1}^n \phi'(|w_{c_j} v_{d^{(i)}}|) v_{d^{(i)}} \epsilon^{(k)} + \right. \\ \left. \frac{1+o(1)}{2n} \phi'(|w_{c_j} \epsilon^{(k)}|) y^{(k)} \|\epsilon^{(k)}\|_2^2 + \right. \\ \left. \frac{1+o(1)}{2n} \sum_{i=1; i \neq k}^n \phi'(|w_{c_j} \epsilon^{(i)}|) y^{(i)} \epsilon^{(i)} \epsilon^{(k)} \right] \end{aligned} \quad (55)$$

$$= \sum_{j=1}^m \frac{1}{m} \left[\frac{1+o(1)}{2n} \sigma^2 \phi'(|w_{c_j} \epsilon^{(k)}|) y^{(k)} + \tau \right] \quad (56)$$

where τ consists of the remaining terms that are negligible since the noise learned by each model is *i.i.d.* and based on

the assumption that $d \gg n^2$. Since the weights learned by different models are as represented in Eq.9, we have,

$$\begin{aligned} \frac{d(w_{avg})}{dt} \epsilon^{(k)} \approx \frac{1+o(1)}{2n} \sigma^2 y^{(k)} \frac{1}{m} \sum_{j=1}^m \phi' \left(\left| \left(\sum_{l=1}^K \alpha_{lj}^t v_l \right. \right. \right. \\ \left. \left. \left. + \sum_{l>K_{cut}^t} y_j^{(l)} \epsilon_j^{(l)} \right) \epsilon^{(k)} \right| \right) \end{aligned} \quad (57)$$

Since the noise $\epsilon^{(i)}$ learned by different models is considered as *i.i.d.*, we get,

$$\begin{aligned} \frac{d(w_{avg})}{dt} \epsilon^{(k)} = \frac{1+o(1)}{2nm} (\sigma^2 y^{(k)} \phi' \left(\left| \sum_{l=1}^K \alpha_{lk}^t v_l \epsilon^{(k)} + \right. \right. \\ \left. \left. \sum_{l>K_{cut}^t} y_k^{(l)} \sigma^2 \right| \right) + \sum_{i=1; i \neq k}^n \phi' \left(\left| \sum_{l=1}^K \alpha_{li}^t v_l \epsilon^{(k)} \right| \right)) \end{aligned} \quad (58)$$

We note that from eq-25, $\sum_{i=1; i \neq k}^n \phi' \left(\left| \sum_{l=1}^K \alpha_{li}^t v_l \epsilon^{(k)} \right| \right) = O\left(\frac{\sigma}{\sqrt{d}}\right)^{q-1}$. Whereas $y_k^{(l)} \sigma^2 = O(1)$. Since it is assumed that $d \gg n^2$. Therefore, we can ignore $\sum_{i=1; i \neq k}^n \phi' \left(\left| \sum_{l=1}^K \alpha_{li}^t v_l \epsilon^{(k)} \right| \right)$. Thus, we get

$$\begin{aligned} \frac{d(w_{avg})}{dt} \epsilon^{(k)} = \frac{1+o(1)}{2nm} \sigma^2 y^{(k)} \phi' \left(\left| \sum_{l=1}^K \alpha_{lk}^t v_l \epsilon^{(k)} + \right. \right. \\ \left. \left. \sum_{l>K_{cut}^t} y_k^{(l)} \sigma^2 \right| \right) \end{aligned} \quad (59)$$

Similarly, we derive the learning dynamics of a single model w_{c_k} below:

$$\begin{aligned} \frac{d(w_{c_k})}{dt} \epsilon^{(k)} = \frac{1+o(1)}{2n} \sigma^2 y^{(k)} \phi' \left(\left| \sum_{l=1}^K \alpha_{lk}^t v_l \epsilon^{(k)} + \right. \right. \\ \left. \left. \sum_{l>K_{cut}^t} y_k^{(l)} \sigma^2 \right| \right) \end{aligned} \quad (60)$$

From Eq.59 and Eq.60, we get the following relation,

$$\frac{1}{m} \frac{d(w_{c_k})}{dt} \epsilon^{(k)} = \frac{d(w_{avg})}{dt} \epsilon^{(k)} \quad (61)$$

In eq-61, we have the rate of change of $w_{avg} = \frac{1}{\epsilon^{(k)} m}$ times the rate of change of w_{c_k} . Therefore the time for convergence for w_{avg} will be $\epsilon^{(k)} m$ times the time for convergence for w_{c_k} , which gives the following as the convergence time for learning the noisy patch, $\epsilon^{(k)}$ by at least one channel $c \in C$ of the model as

$$t = O\left(\frac{nm}{\sigma_0^{q-2} \sigma^q}\right) \quad (62)$$

□

Proposition 3 If the noise learned by each f_θ^k are i.i.d. Gaussian random variables $\sim \mathcal{N}\left(0, \frac{\sigma^2}{d} I_d\right)$, and model weight averaging is performed at epoch T , the convergence time of learning a noisy patch $\epsilon^{(j)}$ in at least one channel $c \in [1, C]$ of the weight averaged model f_θ is given by $T + O\left(\frac{nm^{(q-2)}d^{(q-2)/2}}{\sigma^{(2q-2)}}\right)$ if $d \gg n^2$.

Proof. We assume that the model is close to convergence at epoch T . Hence, its weights can be assumed to be similar to Eq.7. Further, we assume that the weights are composed of noisy and feature patches as shown in Eq.7. Since the noisy patches are assumed to be i.i.d., the standard deviation of the weights corresponding to noisy features is given by $\frac{\sigma}{m\sqrt{d}}$. Thus, using lemma-9 and 9 we get,

$$g(w_c, \epsilon^{(k)}, t = T)^{2-q} = \sigma^{4-2q} m^{q-2} d^{\frac{q-2}{2}} \quad (63)$$

On integrating Eq.49 from time T and substituting the above we get,

$$\begin{aligned} \frac{1 + o(1)}{2n} t \sigma^2 - (q-2) \sigma^{4-2q} m^{q-2} d^{\frac{q-2}{2}} = \\ (2-q)(g(w_c, \epsilon^{(k)}, t = t)^{2-q} \quad (64) \end{aligned}$$

Thus, the convergence time of learning at least one channel $c \in C$ by on using this initialization is given by,

$$t = O\left(\frac{nm^{(q-2)}d^{(q-2)/2}}{\sigma^{(2q-2)}}\right) \quad (65)$$

Further, the total convergence time is given by

$$T + O\left(\frac{nm^{(q-2)}d^{(q-2)/2}}{\sigma^{(2q-2)}}\right) \quad (66)$$

Since we have considered the weights to be composed of two parts, and the model is assumed to be converged with respect to feature patches, such an initialization will not impact their learning dynamics. \square

9.3. Impact of intermediate interpolations

We assume that T in Proposition-3 is negligible with respect to $O\left(\frac{nm^{(q-2)}d^{(q-2)/2}}{\sigma^{(2q-2)}}\right)$. We further analyze the ratio of the convergence time from Proposition-3 (denoted as t) and Proposition-2 (denoted as t'),

$$\frac{t}{t'} = O\left(\frac{m^{q-3}d^{(q-2)/2}\sigma_0^{q-2}}{\sigma^{q-2}}\right) \quad (67)$$

A lower bound on the above equation will occur when $d = n^2$ and $q = 3$. Using this we get,

$$\frac{t}{t'} = O\left(\frac{n\sigma_0}{\sigma}\right) \quad (68)$$

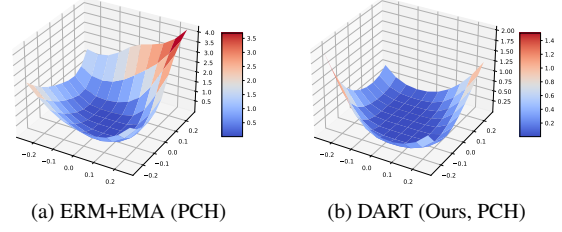


Figure 5. Loss landscape visualization

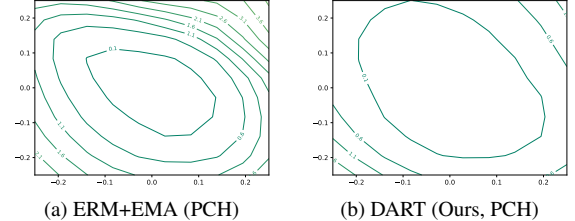


Figure 6. Loss Contour visualization

Thus, the lower bound is of the order n which is greater than 1. Therefore, the convergence time of learning a noisy patch $\epsilon^{(j)}$ in at least one channel $c \in [1, C]$ on performing an intermediate interpolation (Prop.3) is greater than the case where weight-averaging of only final models is performed (Prop.2), by upto $O(n)$.

10. Loss surface plots

We compare the loss surface of the proposed method with ERM training on CIFAR-100 dataset using WRN-28-10 architecture. To exclusively understand the impact of the proposed Diversify-Aggregate-Repeat steps, we present results using the simple augmentations - Pad and Crop followed by Horizontal Flip (PCH) for both ERM and DART. We use exponential moving averaging (EMA) of weights in both the ERM baseline and DART for a fair comparison.

As shown in Fig.5, the loss surface of the proposed method DART is flatter when compared to the ERM baseline. The same is also evident from the level sets of the contour plot in Fig.6. In Table-8, we also use the scale-invariant metrics proposed by Stutz *et al.* [64] to quantitatively verify that the flatness of loss surface is indeed better using the proposed approach DART. Worst Case Flatness represents the Cross-Entropy loss on perturbing the weights in an ℓ_2 norm ball of radius 0.25. Average Flatness represents the Cross-Entropy loss on adding random Gaussian noise with standard deviation 0.25, and further clamping it so that the added noise remains within the ℓ_2 norm ball of radius 0.25. Average Train Loss represents the loss on train set images as shown in Table-8. We achieve lower results when compared to the ERM baseline across all metrics demonstrating that the proposed method DART has a flatter loss landscape

Table 8. **Loss Landscape Sharpness Analysis:** Comparison of the proposed method DART (Pad-Crop) and ERM (Pad-Crop) trained using WRN-28-10 on CIFAR-100. The metrics presented here have been adapted from Stutz *et al.* [64]. For all metrics, a lower value corresponds to a flatter loss landscape.

Method	Worst Case Flatness ↓	Average Flatness ↓	Average Train Loss ↓
ERM (Pad+Crop)	4.173	1.090	0.0028
DART (Pad+Crop) (Ours)	2.037	0.294	0.0022

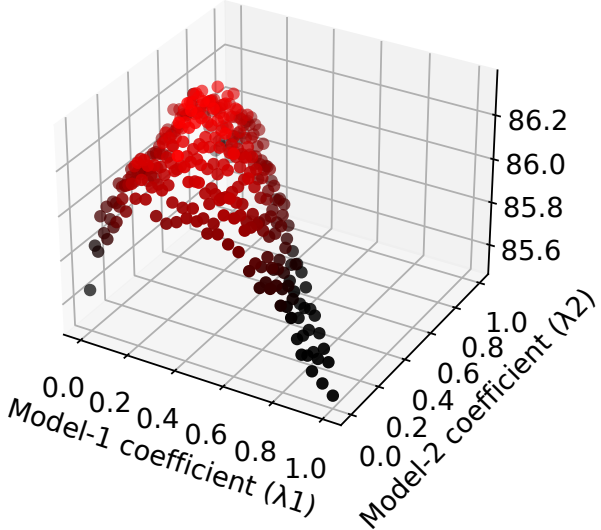


Figure 7. **Accuracy (%) on interpolating the final converged models trained using DART (ours)** using WRN-28-10 model and CIFAR-100 dataset, by taking their convex combination. Maximum accuracy of 86.33 is obtained on interpolating, using three experts with accuracies 85.65, 85.75 and 85.51. For the best setting, $\lambda_1 = 0.17$ and $\lambda_2 = 0.46$.

compared to ERM.

11. Additional Results: In-Domain generalization setting

11.1. Model coefficients

While in the proposed method, we give equal weight to all branches, we note that fine-tuning this in a greedy manner [75] can give a further boost in accuracy. As shown in Fig.7, the best accuracy obtained is 86.33% at $\lambda_1 = 0.17$, $\lambda_2 = 0.46$, when compared to 86.24% with $\lambda_1 = \lambda_2 = 0.33$. These results are lower than those reported in Tables-2 and 9 of the main paper since the runs in Fig.7 do not use EMA, while our main method does.

11.2. Training plots

We show the training plots for In-domain generalization training of CIFAR-100 on WRN-28-10 in Fig.8. We firstly note that not only does our method yield gains on the final interpolation step (as seen in Tables-2, 9 in the main paper), but the step of intermediate interpolation ensures that the individual models are also better than the ERM baselines trained using the respective augmentations. Specifically, while the initial interpolations help in bringing the models closer to each other in the loss landscape, the later ones actually result in performance gains, since the low learning rate ensures that the flatter loss surface obtained using intermediate weight averaging is retained.

12. Details on Domain Generalization

12.1. Training Details

Since the domain shift across individual domains is larger in the Domain Generalization setting when compared to the In-Domain generalization setting, we found that training individual branches on a mix of all domains was better than training each branch on a single domain. Moreover, training on a mix of all domains also improves the individual branch accuracy, thereby boosting the accuracy of the final interpolated model. We train 4 branches (6 for DomainNet), where one branch is trained with an equal proportion of all domains, while the other three branches are allowed to be experts on individual domains by using a higher fraction (40% for DomainNet and 50% for other datasets) of the selected domain for the respective branch.

In the Domain Generalization setting, the step of explicitly training on mixed augmentations/ domains (L4-L5 in Algorithm-1 of the main paper) is replaced by the initialization of the model using ImageNet pretrained weights, which ensures that all models are in the loss basin. Moreover, this also helps in reducing the overall compute.

For the results presented in the Tables 12.3.1, 12.3.2, 12.3.3, 12.3.4, 12.3.5, 12.3.6 and Table-3 of the main paper, the training configuration of (training iterations, interpolation frequency) was set to (15k, 1k) for DomainNet and (10k, 1k) for all other datasets, whereas for the results presented in Table-4 of the main paper, the configuration was set to (5k, 600) for DANN [21] and CDANN [44], and (8k, 1k) for the rest, primarily to reduce compute. The difference in adversarial training approaches (DANN and CDANN) was primarily because their training is not stable for longer training iterations. SWAD-specific hyperparameters were set as suggested by the authors [6] without additional tuning. Although the proposed approach uses higher compute than the baselines, we show in Fig.9(a) that even with higher compute, the baselines cannot achieve better performance. Although we compare with comparable compute for the In-Domain generalization setting (Tables-2, 9 in the main pa-

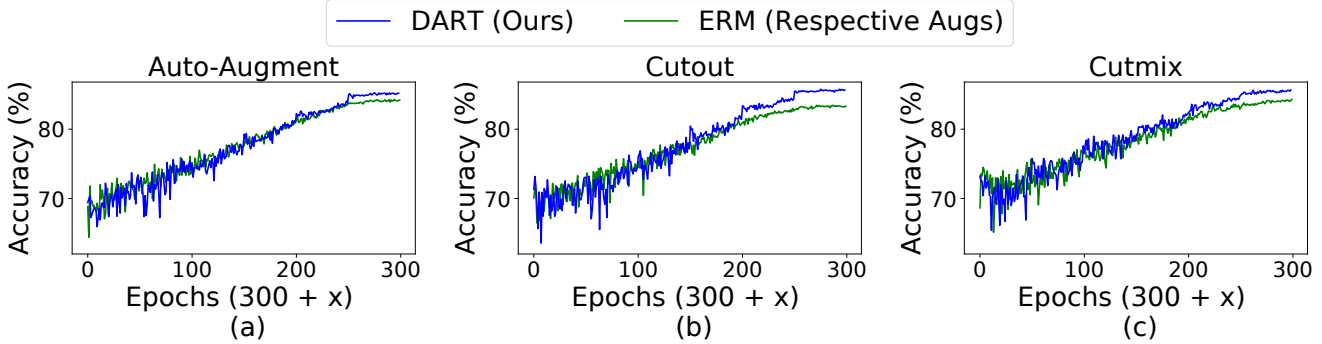


Figure 8. **Comparison of the test accuracy (%) of ERM training using different augmentations with the respective augmentation expert of DART** on CIFAR-100, WRN-28-10. The analysis is done from 300 epochs onwards. Most of the gains of the proposed method occur at the end of training, when learning rate is low and the experts are present within a common basin.

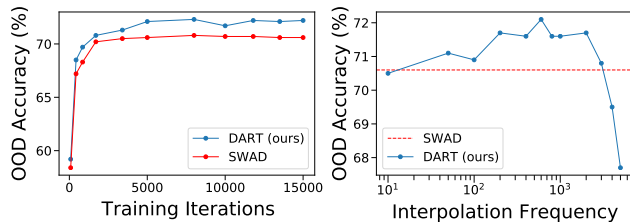


Figure 9. **Performance of DART across (a) varying training iterations and (b) varying interpolation frequency:** (a) compares the proposed method DART’s performance with the SWAD baseline when trained for higher number of iterations. Interpolation frequency was maintained such that the number of interpolations remained same (8) in every case. (b) demonstrates the effect of intermediate interpolation frequency on DART. The training iterations were kept constant (5k).

per), for the Domain Generalization setting we report the baselines from DomainBed [24] and the respective papers as is the common practice.

12.2. Ablation experiments

We present ablation experiments on the Office-Home dataset in Fig.9. We present average accuracy across all domain splits as is common practice in Domain Generalization [24].

Variation across training compute: Fig.9 (a) demonstrates that the performance of SWAD plateaus early compared to DART, when trained for a higher number of training iterations. We note that DART achieves a significant improvement in the saturating accuracy over the baseline. This indicates that although the proposed method requires higher compute, DART trades it off for improved performance.

Variation in interpolation frequency: Fig.9 (b) describes the impact of varying the interpolation frequency in the proposed method DART. The number of training iterations is set to 5k for this experiment. We note that the accuracy is stable across a wide range of interpolation frequencies (x-axis is in log scale). This shows that the pro-

Table 9. **Different model architectures:** Performance (%) of DART when compared to Mixed-Training (MT) across different architectures. Standard deviation is reported across 5 reruns.

Model	Method	CIFAR-10	CIFAR-100
ResNet18	ERM+EMA (Mixed - MT)	97.08 ± 0.05	82.25 ± 0.29
	DART (Ours)	97.14 ± 0.08	82.89 ± 0.07
WRN-28-10	ERM+EMA (Mixed - MT)	97.76 ± 0.17	85.57 ± 0.13
	DART (Ours)	97.96 ± 0.06	86.46 ± 0.12

Table 10. **OOD Performance:** Performance (%) of DART using Pad+Crop+HFlip (PCH) augmentations across all branches, when compared to ERM training, on the corruptions datasets CIFAR10-C and CIFAR100-C using WideResNet-28-10 model. Standard deviation is reported across 5 reruns

Method	CIFAR-10	CIFAR10-C	CIFAR-100	CIFAR100-C
ERM+EMA (PCH)	96.41 ± 0.13	77.56 ± 0.15	81.67 ± 0.08	54.22 ± 0.11
DART (Ours, PCH)	96.64 ± 0.11	78.25 ± 0.17	82.31 ± 0.18	55.05 ± 0.13

posed method is not very sensitive to the frequency of interpolation, and does not require fine-tuning for every dataset. We therefore use the same interpolation frequency of 1k for all the datasets and training splits of DomainBed. We note that the proposed method performs better than baseline in all cases except when the frequency is kept too low (≈ 10) or too high (close to total training iterations). The sharp deterioration in performance in the case of no intermediate interpolation (interpolation frequency = total training steps) illustrates the necessity of intermediate interpolation in the proposed method.

Evaluation across different model capacities: We present results on ResNet-18 and WideResNet-28-10 in Table-9. The gains obtained on WideResNet-28-10 are larger (0.2 and 0.89) when compared to ResNet-18 (0.06 and 0.64) demonstrating the scalability of our method.

Out-Of-Distribution (OOD) performance: We compare the performance of DART w.r.t. the ERM+EMA baseline on the Common Corruptions datasets CIFAR-10-C and

CIFAR-100-C [26] in Table-10. While SOTA approaches on these datasets utilize different augmentations for training [27], our goal here is to merely show that the proposed approach improves OOD performance as well, and hence choose the simple augmentation Pad, Crop, and Horizontal Flip for this run. This also ensures that the train and test distributions are truly non-overlapping. We obtain improvements of 0.23% and 0.64% on In-Domain test set and 0.69% and 0.83% on OOD test sets of CIFAR-10 and CIFAR-100 datasets respectively, demonstrating that the proposed approach improves both ID and OOD generalization.

12.3. Detailed Results

In this section, we present complete Domain Generalization results (Out-of-domain accuracies %) on VLCS (Table-12.3.2), PACS (Table-12.3.3), OfficeHome (Table-12.3.4), TerraIncognita (Table-12.3.5) and DomainNet (Table-12.3.6) benchmarks. We also present the average accuracy across all domain splits and datasets in Table-12.3.1. We note that the proposed method DART when combined with SWAD [6] outperforms all existing methods across all datasets. All the tables are presented in the following page.

12.3.1 Averages

Algorithm	VLCS	PACS	OfficeHome	TerraIncognita	DomainNet	Avg
ERM [67]	77.5 ± 0.4	85.5 ± 0.2	66.5 ± 0.3	46.1 ± 1.8	40.9 ± 0.1	63.3
IRM [2]	78.5 ± 0.5	83.5 ± 0.8	64.3 ± 2.2	47.6 ± 0.8	33.9 ± 2.8	61.6
GroupDRO [58]	76.7 ± 0.6	84.4 ± 0.8	66.0 ± 0.7	43.2 ± 1.1	33.3 ± 0.2	60.7
Mixup [73]	77.4 ± 0.6	84.6 ± 0.6	68.1 ± 0.3	47.9 ± 0.8	39.2 ± 0.1	63.4
MLDG [41]	77.2 ± 0.4	84.9 ± 1.0	66.8 ± 0.6	47.7 ± 0.9	41.2 ± 0.1	63.6
CORAL [65]	78.8 ± 0.6	86.2 ± 0.3	68.7 ± 0.3	47.6 ± 1.0	41.5 ± 0.1	64.5
MMD [43]	77.5 ± 0.9	84.6 ± 0.5	66.3 ± 0.1	42.2 ± 1.6	23.4 ± 9.5	58.8
DANN [21]	78.6 ± 0.4	83.6 ± 0.4	65.9 ± 0.6	46.7 ± 0.5	38.3 ± 0.1	62.6
CDANN [44]	77.5 ± 0.1	82.6 ± 0.9	65.8 ± 1.3	45.8 ± 1.6	38.3 ± 0.3	62.0
MTL [4]	77.2 ± 0.4	84.6 ± 0.5	66.4 ± 0.5	45.6 ± 1.2	40.6 ± 0.1	62.9
SagNet [48]	77.8 ± 0.5	86.3 ± 0.2	68.1 ± 0.1	48.6 ± 1.0	40.3 ± 0.1	64.2
ARM [82]	77.6 ± 0.3	85.1 ± 0.4	64.8 ± 0.3	45.5 ± 0.3	35.5 ± 0.2	61.7
VREx [39]	78.3 ± 0.2	84.9 ± 0.6	66.4 ± 0.6	46.4 ± 0.6	33.6 ± 2.9	61.9
RSC [31]	77.1 ± 0.5	85.2 ± 0.9	65.5 ± 0.9	46.6 ± 1.0	38.9 ± 0.5	62.7
SWAD [6]	79.1 ± 0.1	88.1 ± 0.1	70.6 ± 0.2	50.0 ± 0.3	46.5 ± 0.1	66.9
DART w/o SWAD (ours)	78.5 ± 0.7	87.3 ± 0.5	70.1 ± 0.2	48.7 ± 0.8	45.8	66.1
DART w/ SWAD (ours)	80.3 ± 0.2	88.9 ± 0.1	71.9 ± 0.1	51.3 ± 0.2	47.2	67.9

12.3.2 VLCS

Algorithm	C	L	S	V	Avg
ERM	97.7 ± 0.4	64.3 ± 0.9	73.4 ± 0.5	74.6 ± 1.3	77.5
IRM	98.6 ± 0.1	64.9 ± 0.9	73.4 ± 0.6	77.3 ± 0.9	78.5
GroupDRO	97.3 ± 0.3	63.4 ± 0.9	69.5 ± 0.8	76.7 ± 0.7	76.7
Mixup	98.3 ± 0.6	64.8 ± 1.0	72.1 ± 0.5	74.3 ± 0.8	77.4
MLDG	97.4 ± 0.2	65.2 ± 0.7	71.0 ± 1.4	75.3 ± 1.0	77.2
CORAL	98.3 ± 0.1	66.1 ± 1.2	73.4 ± 0.3	77.5 ± 1.2	78.8
MMD	97.7 ± 0.1	64.0 ± 1.1	72.8 ± 0.2	75.3 ± 3.3	77.5
DANN	99.0 ± 0.3	65.1 ± 1.4	73.1 ± 0.3	77.2 ± 0.6	78.6
CDANN	97.1 ± 0.3	65.1 ± 1.2	70.7 ± 0.8	77.1 ± 1.5	77.5
MTL	97.8 ± 0.4	64.3 ± 0.3	71.5 ± 0.7	75.3 ± 1.7	77.2
SagNet	97.9 ± 0.4	64.5 ± 0.5	71.4 ± 1.3	77.5 ± 0.5	77.8
ARM	98.7 ± 0.2	63.6 ± 0.7	71.3 ± 1.2	76.7 ± 0.6	77.6
VREx	98.4 ± 0.3	64.4 ± 1.4	74.1 ± 0.4	76.2 ± 1.3	78.3
RSC	97.9 ± 0.1	62.5 ± 0.7	72.3 ± 1.2	75.6 ± 0.8	77.1
SWAD	98.8 ± 0.1	63.3 ± 0.3	75.3 ± 0.5	79.2 ± 0.6	79.1
DART w/o SWAD	97.9 ± 1.0	64.2 ± 0.7	73.9 ± 1.1	78.1 ± 1.6	78.5
DART w/ SWAD	98.7 ± 0.0	66.4 ± 0.3	75.8 ± 0.6	80.4 ± 0.3	80.3

12.3.3 PACS

Algorithm	A	C	P	S	Avg
ERM	84.7 ± 0.4	80.8 ± 0.6	97.2 ± 0.3	79.3 ± 1.0	85.5
IRM	84.8 ± 1.3	76.4 ± 1.1	96.7 ± 0.6	76.1 ± 1.0	83.5
GroupDRO	83.5 ± 0.9	79.1 ± 0.6	96.7 ± 0.3	78.3 ± 2.0	84.4
Mixup	86.1 ± 0.5	78.9 ± 0.8	97.6 ± 0.1	75.8 ± 1.8	84.6
MLDG	85.5 ± 1.4	80.1 ± 1.7	97.4 ± 0.3	76.6 ± 1.1	84.9
CORAL	88.3 ± 0.2	80.0 ± 0.5	97.5 ± 0.3	78.8 ± 1.3	86.2
MMD	86.1 ± 1.4	79.4 ± 0.9	96.6 ± 0.2	76.5 ± 0.5	84.6
DANN	86.4 ± 0.8	77.4 ± 0.8	97.3 ± 0.4	73.5 ± 2.3	83.6
CDANN	84.6 ± 1.8	75.5 ± 0.9	96.8 ± 0.3	73.5 ± 0.6	82.6
MTL	87.5 ± 0.8	77.1 ± 0.5	96.4 ± 0.8	77.3 ± 1.8	84.6
SagNet	87.4 ± 1.0	80.7 ± 0.6	97.1 ± 0.1	80.0 ± 0.4	86.3
ARM	86.8 ± 0.6	76.8 ± 0.5	97.4 ± 0.3	79.3 ± 1.2	85.1
VREx	86.0 ± 1.6	79.1 ± 0.6	96.9 ± 0.5	77.7 ± 1.7	84.9
RSC	85.4 ± 0.8	79.7 ± 1.8	97.6 ± 0.3	78.2 ± 1.2	85.2
DMG	82.6	78.1	94.3	78.3	83.4
MetaReg	87.2	79.2	97.6	70.3	83.6
DSON	87.0	80.6	96.0	82.9	86.6
SWAD	89.3 ± 0.2	83.4 ± 0.6	97.3 ± 0.3	78.2 ± 0.5	88.1
DART w/o SWAD	87.1 ± 1.5	83.5 ± 0.9	96.9 ± 0.3	81.8 ± 0.9	87.3
DART w/ SWAD	90.1 ± 0.1	84.5 ± 0.2	97.7 ± 0.2	83.4 ± 0.1	88.9

12.3.4 OfficeHome

Algorithm	A	C	P	R	Avg
ERM	61.3 ± 0.7	52.4 ± 0.3	75.8 ± 0.1	76.6 ± 0.3	66.5
IRM	58.9 ± 2.3	52.2 ± 1.6	72.1 ± 2.9	74.0 ± 2.5	64.3
GroupDRO	60.4 ± 0.7	52.7 ± 1.0	75.0 ± 0.7	76.0 ± 0.7	66.0
Mixup	62.4 ± 0.8	54.8 ± 0.6	76.9 ± 0.3	78.3 ± 0.2	68.1
MLDG	61.5 ± 0.9	53.2 ± 0.6	75.0 ± 1.2	77.5 ± 0.4	66.8
CORAL	65.3 ± 0.4	54.4 ± 0.5	76.5 ± 0.1	78.4 ± 0.5	68.7
MMD	60.4 ± 0.2	53.3 ± 0.3	74.3 ± 0.1	77.4 ± 0.6	66.3
DANN	59.9 ± 1.3	53.0 ± 0.3	73.6 ± 0.7	76.9 ± 0.5	65.9
CDANN	61.5 ± 1.4	50.4 ± 2.4	74.4 ± 0.9	76.6 ± 0.8	65.8
MTL	61.5 ± 0.7	52.4 ± 0.6	74.9 ± 0.4	76.8 ± 0.4	66.4
SagNet	63.4 ± 0.2	54.8 ± 0.4	75.8 ± 0.4	78.3 ± 0.3	68.1
ARM	58.9 ± 0.8	51.0 ± 0.5	74.1 ± 0.1	75.2 ± 0.3	64.8
VREx	60.7 ± 0.9	53.0 ± 0.9	75.3 ± 0.1	76.6 ± 0.5	66.4
RSC	60.7 ± 1.4	51.4 ± 0.3	74.8 ± 1.1	75.1 ± 1.3	65.5
SWAD	66.1 ± 0.4	57.7 ± 0.4	78.4 ± 0.1	80.2 ± 0.2	70.6
DART w/o SWAD	64.3 ± 0.2	57.9 ± 0.9	78.3 ± 0.6	79.9 ± 0.1	70.1
DART w/ SWAD	67.1 ± 0.2	59.2 ± 0.1	79.7 ± 0.1	81.5 ± 0.1	71.9

12.3.5 TerraIncognita

Algorithm	L100	L38	L43	L46	Avg
ERM	49.8 ± 4.4	42.1 ± 1.4	56.9 ± 1.8	35.7 ± 3.9	46.1
IRM	54.6 ± 1.3	39.8 ± 1.9	56.2 ± 1.8	39.6 ± 0.8	47.6
GroupDRO	41.2 ± 0.7	38.6 ± 2.1	56.7 ± 0.9	36.4 ± 2.1	43.2
Mixup	59.6 ± 2.0	42.2 ± 1.4	55.9 ± 0.8	33.9 ± 1.4	47.9
MLDG	54.2 ± 3.0	44.3 ± 1.1	55.6 ± 0.3	36.9 ± 2.2	47.7
CORAL	51.6 ± 2.4	42.2 ± 1.0	57.0 ± 1.0	39.8 ± 2.9	47.6
MMD	41.9 ± 3.0	34.8 ± 1.0	57.0 ± 1.9	35.2 ± 1.8	42.2
DANN	51.1 ± 3.5	40.6 ± 0.6	57.4 ± 0.5	37.7 ± 1.8	46.7
CDANN	47.0 ± 1.9	41.3 ± 4.8	54.9 ± 1.7	39.8 ± 2.3	45.8
MTL	49.3 ± 1.2	39.6 ± 6.3	55.6 ± 1.1	37.8 ± 0.8	45.6
SagNet	53.0 ± 2.9	43.0 ± 2.5	57.9 ± 0.6	40.4 ± 1.3	48.6
ARM	49.3 ± 0.7	38.3 ± 2.4	55.8 ± 0.8	38.7 ± 1.3	45.5
VREx	48.2 ± 4.3	41.7 ± 1.3	56.8 ± 0.8	38.7 ± 3.1	46.4
RSC	50.2 ± 2.2	39.2 ± 1.4	56.3 ± 1.4	40.8 ± 0.6	46.6
SWAD	55.4 ± 0.0	44.9 ± 1.1	59.7 ± 0.4	39.9 ± 0.2	50.0
DART w/o SWAD	54.6 ± 1.1	44.9 ± 1.6	58.7 ± 0.5	36.6 ± 1.9	48.7
DART w/ SWAD	56.3 ± 0.4	47.1 ± 0.3	61.2 ± 0.3	40.5 ± 0.1	51.3

12.3.6 DomainNet

Algorithm	clip	info	paint	quick	real	sketch	Avg
ERM	58.1 \pm 0.3	18.8 \pm 0.3	46.7 \pm 0.3	12.2 \pm 0.4	59.6 \pm 0.1	49.8 \pm 0.4	40.9
IRM	48.5 \pm 2.8	15.0 \pm 0.5	38.3 \pm 4.3	10.9 \pm 0.5	48.2 \pm 5.2	42.3 \pm 3.1	33.9
GroupDRO	47.2 \pm 0.5	17.5 \pm 0.4	33.8 \pm 0.5	9.3 \pm 0.3	51.6 \pm 0.4	40.1 \pm 0.6	33.3
Mixup	55.7 \pm 0.3	18.5 \pm 0.5	44.3 \pm 0.5	12.5 \pm 0.4	55.8 \pm 0.3	48.2 \pm 0.5	39.2
MLDG	59.1 \pm 0.2	19.1 \pm 0.3	45.8 \pm 0.7	13.4 \pm 0.3	59.6 \pm 0.2	50.2 \pm 0.4	41.2
CORAL	59.2 \pm 0.1	19.7 \pm 0.2	46.6 \pm 0.3	13.4 \pm 0.4	59.8 \pm 0.2	50.1 \pm 0.6	41.5
MMD	32.1 \pm 13.3	11.0 \pm 4.6	26.8 \pm 11.3	8.7 \pm 2.1	32.7 \pm 13.8	28.9 \pm 11.9	23.4
DANN	53.1 \pm 0.2	18.3 \pm 0.1	44.2 \pm 0.7	11.8 \pm 0.1	55.5 \pm 0.4	46.8 \pm 0.6	38.3
CDANN	54.6 \pm 0.4	17.3 \pm 0.1	43.7 \pm 0.9	12.1 \pm 0.7	56.2 \pm 0.4	45.9 \pm 0.5	38.3
MTL	57.9 \pm 0.5	18.5 \pm 0.4	46.0 \pm 0.1	12.5 \pm 0.1	59.5 \pm 0.3	49.2 \pm 0.1	40.6
SagNet	57.7 \pm 0.3	19.0 \pm 0.2	45.3 \pm 0.3	12.7 \pm 0.5	58.1 \pm 0.5	48.8 \pm 0.2	40.3
ARM	49.7 \pm 0.3	16.3 \pm 0.5	40.9 \pm 1.1	9.4 \pm 0.1	53.4 \pm 0.4	43.5 \pm 0.4	35.5
VREx	47.3 \pm 3.5	16.0 \pm 1.5	35.8 \pm 4.6	10.9 \pm 0.3	49.6 \pm 4.9	42.0 \pm 3.0	33.6
RSC	55.0 \pm 1.2	18.3 \pm 0.5	44.4 \pm 0.6	12.2 \pm 0.2	55.7 \pm 0.7	47.8 \pm 0.9	38.9
MetaReg	59.8	25.6	50.2	11.5	64.6	50.1	43.6
DMG	65.2	22.2	50.0	15.7	59.6	49.0	43.6
SWAD	66.0 \pm 0.1	22.4 \pm 0.3	53.5 \pm 0.1	16.1 \pm 0.2	65.8 \pm 0.4	55.5 \pm 0.3	46.5
DART w/o SWAD	65.9	21.9	52.6	15.1	64.9	54.3	45.8
DART w/ SWAD	66.5	22.8	54.2	16.1	67.3	56.3	47.2